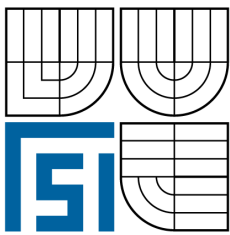# VYSOKÉ UČENÍ TECHNICKÉ V BRNĚ
BRNO UNIVERSITY OF TECHNOLOGY

FAKULTA STROJNÍHO INŽENÝRSTVÍ
ÚSTAV MECHANIKY TĚLES, MECHATRONIKY A BIOMECHANIKY

FACULTY OF MECHANICAL ENGINEERING
INSTITUTE OF SOLID MECHANICS, MECHATRONICS AND BIOMECHANICS

MODELING AND SIMULATION OF MOBILE WORKING MACHINE POWERTRAIN
MODELOVÁNÍ A SIMULACE POHONU MOBILNÍHO PRACOVNÍHO STROJE

DIPLOMOVÁ PRÁCE
MASTER'S THESIS

AUTOR PRÁCE   Bc. PETER ZAVADINKA
AUTHOR

VEDOUCÍ PRÁCE   doc. Ing. PETER KRIŠŠÁK, Ph.D.
SUPERVISOR

BRNO 2009

Vysoké učení technické v Brně, Fakulta strojního inženýrství

Ústav mechaniky těles, mechatroniky a biomechaniky
Akademický rok: 2008/09

ZADÁNÍ DIPLOMOVÉ PRÁCE

student(ka): Zavadinka Peter, Bc.

který/která studuje v **magisterském studijním programu**

obor: **Mechatronika (3906T001)**

Ředitel ústavu Vám v souladu se zákonem č.111/1998 o vysokých školách a se Studijním a zkušebním řádem VUT v Brně určuje následující téma diplomové práce:

Modelování a simulace pohonu mobilního pracovního stroje

v anglickém jazyce:

Automotive Control of mobile working Machine

Stručná charakteristika problematiky úkolu:

Automatické řízení (AC-Automotive control) je logický vývojový stupeň pro poskytování budoucích řešení AC pro stále rostoucí automatizační trh mobilních pracovních strojů. Nejrychlejší růst AC trhu v rámci mobilních pracovních strojů dosahuje řešení na základě EH (electro-hydraulic) řízení. Řízení je připraveno na další vývojový stupeň, tedy na řízení se zaměřením na implementaci norem a předpisů, jako např. TIER 4 (regulace emisí). AC aplikace nabízené společností Sauer-Danfoss mají největší potenciál růstu v rámci klíčových aplikací HST (Hydro-Static-Transmision). V období let 2008-2012 se předpokladá přechod technologie řízení, např. z důvodu regulací emisí, z hydraulického AC na EH AC. V současné době jsou na trhu pouze integrované elektronické AC produkty společnosti S-D ale schopnost poskytnout novou architekturu řízení vozidla umožňuje změnit současnou situaci na trhu mobilních pracovních strojů směrem k očekáváním trendům. Projekt sestává z vytvoření dynamického modelu mobilního pracovního stroje a návrhu vhodného algoritmu řízení pro motor a hydraulické prvky v závislosti na pracovních podmínkách.

Cíle diplomové práce:

Cílem práce je navrhnout algoritmus řízení vybraného mobilního pracovního stroje v závislosti na pracovních podmínkách. Navržený algoritmus má sloužit pro vývojové aktivity výrobce mobilního pracovního stroje.

Seznam odborné literatury:

[1] FITCH, E. C., HONG, I. T.: Hydraulic System Modeling and Simulation. Seminar Version, Published by BarDyne, Inc., 2001, 290 p..

[2] HARISSON, H. R., NETTLETON, T.: Advanced Engineering Dynamics. Published by Arnold, 1997, ISBN 0 340 64571 7, 301 p.

[3] KUČÍK, P., STRÁŽOVEC, I., KRIŠŠÁK, P.: Hydraulický prenos energie – mobilné pracovné stroje. Vydala Žilinská univerzita v Žiline, vydavatežstvo EDIS, 2000, ISBN 80-7100-725-0, 384 p.

[4] MANRING, N., D.: Hydraulic Control Systems. Published by John Wiley & Sons, Inc., 2005, 446 p.

[5] Sauer – Danfoss catalogues.

Vedoucí diplomové práce: doc. Ing. Peter Kriššak, Ph.D.

Termín odevzdání diplomové práce je stanoven časovým plánem akademického roku 2008/09.

V Brně, dne 26.11.2008

L.S.

prof. Ing. Jindřich Petruška, CSc.
Ředitel ústavu

doc. RNDr. Miroslav Doupovec, CSc.
Děkan fakulty

Abstract

Modeling and simulation of mobile working machine powertrain

This thesis deals with dynamic model creation of four wheel drive mobile working machine. The goal of the thesis is to create powertrain model of mobile working machine. The hydrostatic transmission part of the model was supplied by the Sauer-Danfoss company. The model of mobile working machine was created in MATLAB-Simulink environment. The thesis is also devoted to selection of hydrostatic transmission control type and design of control algorithm. An output is mathematical and physical powertrain model of four wheel drive mobile working machine with hydrostatic transmission control algorithm in MATLAB-Simulink environment.

Key words: mobile working machine, powertrain, hydrostatic transmission, control algorithm, simulation, modeling, model, MATLAB-Simulink

Abstrakt

Modelovanie a simulácia pohonu mobilného pracovného stroja

Táto diplomová práca sa zaoberá vytvorením dynamického modelu mobilného pracovného stroja. Cieľom práce je vytvorenie blokového modelu pohonu štvorkolesového mobilného pracovného stroja. Model hydrostatického prevodu bol dodaný firmou Sauer-Danfoss. Model mobilného pracovného stroja bol vytvorený v programe MATLAB-Simulink. Dalšou časťou práce je výber typu riadenia hydrostatického prevodu a návrh riadiaceho algoritmu hydrostatického prevodu. Výstupom práce je blokový matematicko-fyzikálny model pohonu štvorkolesového mobilného pracovného stroja spolu s riadiacim algoritmom hydrostatického prevodu v prostredí MATLAB-Simulink.

Kľúčové slová: mobilný pracovný stroj, pohon, hydrostatická prevodovka, riadiaci algoritmus, simulácia, modelovanie, model, MATLAB-Simulink

Statutory declaration

With this statement I claim, that this thesis is my genuine authorial thesis, which was created under leadership of my master thesis leader and with usage of mentioned references.

Peter Zavadinka, Brno, 2009

Acknowledgement

Contents

1 Introduction

A shortening of the product development time indicates a significant progress over the last decade. However there are still capabilities for improvement in this product development sphere. One of them is application of mechatronics, which can give producers decisive trading advantage.

The mechatronics is an integration of electrotechnical, mechanical, hydraulic, pneumatic, control and computer systems knowledge during product development and manufacturing. The mechatronics uses combination of actuators, sensors, control systems and computers in order to obtain synergic effect. The application of mechatronics achieves short development time, reduces costs, increases quality, safety and performance. It comes out from definition that it is necessary for this field to have basic knowledge from various technical disciplines and possibility of team co-operation.

The basic tool for development of mechatronics products is computer simulation. Generally the computer simulation allows primary to reduce time and development costs of new product. A growth of the computing power and accessibility of specialized software make complex simulations possible and subsequently prepare conditions for mechatronics that considers the product complexly. It can be assumed, that the mechatronics will obtain more importance with gradual hardware and software development for computer simulations.

Modern mobile working machines are integration of mechanical, hydraulic, pneumatic, electric and electronic systems. Therefore they belong to mechatronics products as well as each modern product.

The computer simulations in the mobile working machine industry belong to main tools by development of the new product. The computer simulations provide mainly testing of new ideas, various working conditions, systems and control algorithms. They predict behavior of whole system even before the first prototype of new product is created or tested. An optimization is reason for using simulations too. The optimization process is aimed to decreasing of production and operating costs. At last years a subject of interest is also decreasing of environment load.

Despite of fast development of computational tolls it is the simulation engineer, who has to solve technical part of the simulated problem. It is about searching of compromise between model complexity, speed, model accuracy and stability. This thesis tries to describe one of the possible ways how to design controls of mobile working machines.

2   Problem formulation and thesis goals

2.1   Problem formulation

Typical features of mobile working machine powertrain is energy transfer from energy source to energy consumer and energy conversion during this transfer, energy loses are important mainly from economic and ecological point of view.

The hydrostatic transmission (HST) control of mobile working machine (MWS) allows influencing of vehicle's operating characteristics. It means effective energy utilization.
A properly designed HST control algorithm reduces fuel consumption, emission and operation costs of MWM with preservation of required power during working mode.

Mobile working machines work in the several modes. Each mode is oriented to different operation factor. Most frequently it is fuel consumption and power. From physical dependence between fuel consumption and power it comes out that the control algorithm design is based on searching compromise between power and fuel consumption in specific working mode. For this reason the control algorithm design of MWM is difficult and requires complex approach.

In most cases it is necessary to crate dynamic model of MWM. Its creation is determined by extensive knowledge of vehicle's physical behavior.

2.2   Thesis goals

- Creation of four wheel drive model of mobile working machine with modular structure in MATLAB-Simulink enviroment.

- Design of hydrostatic transmission control algorithm of mobile working machine.

- Simulation and analyzing of various working conditions of selected mobile working machine.

3 Mobile working machines (MWM)

If we take a look at theory of cars and trucks in comparison with mobile working machines we find out that not many authors write about mobile working machines as about complex systems. Mobile working machines focused on hydraulic energy transfer are analyzed mainly by Kučík, Strážovec and Kriššák [14]. Baver [2] deals with agriculture mobile working machines. There were used mainly references [14], [2], [13], [12], [20], and [21] in this chapter.

3.1 Definition and decomposition of mobile working machines

The mobile working machine is machine intended for a transport and material manipulation. This machine is equipped with mobile chassis, which allows machine's movement in terrain but also on public roads with higher than technological speed.

The mobile working machines can be divided by several standards [14]. For example by type of chassis:

- Wheeled.
- Crawler.
- Walking.

Another standard is application of MWM:

- Building, road-building and ground machines.
- Transport machinery and vehicles equipped with work functions.
- Forest and agriculture machines.
- Rail mobile working machines.
- Military and other special machines.

It is possible to find more information in reference [14].

A design of mobile working machines is very different and depends on the type and application of MWM [14]. Basically each MWM consists of:

- Engine with equipment.
- Gear mechanism.
- Driving and steering mechanism.

- Work functions.
- Control mechanism.
- Operator workstation.

3.2   Energy transfer and energy conversion

Definitions of following terms are important for physical model analysis [14].

Powertrain is a device intended for machine or machine part actuation with final specified movement state. In general: In all the types of powertrains is energy transfer or energy conversion.

Energy transfer is transfer of energy from place of energy abundance (source, engine) to place of energy consumption (machine wheel) in the delimitated part of the area. This area is intended and created for this purpose. There are also special cases of energy transfer (from wheel to engine). These cases, occurring by special working conditions, are analyzed in another chapter.

Energy conversion is a process of physical energy conversion to another form. For example in the combustion engine (CE) it is conversion from chemical to mechanical form or in the pump it is conversion from mechanical to hydraulic form. The energy conversion is usually related with change of power (energy) carrier.

Power (energy) converter is a device, which performs energy conversion from one energy type to a another energy type. The energy conversion is typical for mechatronic systems. An analogy between hydraulic and electrical systems could be found. Some hydraulic machines can act like generators or motors as well as some electrical machines. A working mode determination depends on direction of the energy transfer. The direction of energy transfer is not exactly determinated. For example motor can act like generator in special conditions and generator can act like motor.

Energy transfer is a process, by which transferred energy is converted from one energy carrier to another energy carrier where these carriers could by same or different. There are energy losses in areas of the transfer. These losses are mainly caused by energy conversion to unwanted heat eventually it can be caused by energy carrier loss (in the hydraulic systems the carrier loss is caused by leakage).

3.3 Configuration of mobile working machine powertrain

The typical configuration of most MWM is shown in Figure 3.1. The powertrain of MWM consists of three basic parts [14]:

- Source of mechanical energy with equipment.
- Gear mechanism with equipment.
- Control system with equipment.
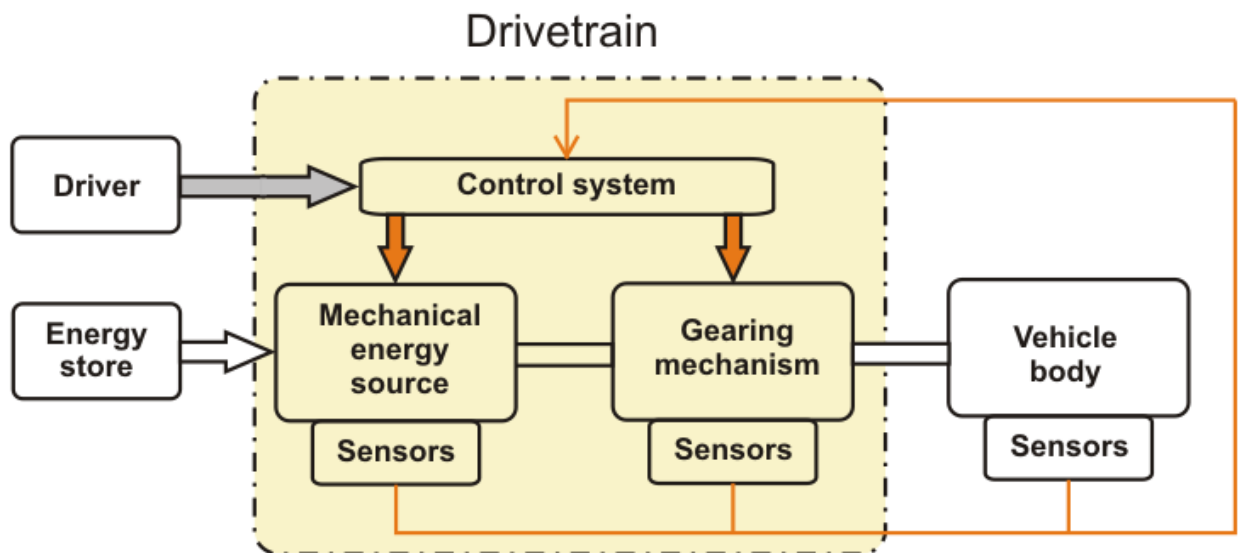
Figure 3.1: Basic parts of MWM powertrain

Source of mechanical energy - driving engine is a technical device, which performs a task of mechanical energy source. It is power converter in which the energy from source (diesel, petrol, gas and electric energy) is converted to mechanical energy. The most commonly used driving engine is diesel four-stroke engine eventually petrol engine or electric motor. A usage range of diesel engine or another driving engine type is very limited. For this reason an application of the gear mechanism is necessary.

Mechanical energy source of MWM is also used as the power source for work functions of the machine. The gear mechanism is also used for energy distribution from engine to output powertrain components. These components are driving wheels, linear hydromotors of work functions and other energy consumers [14].

Gear mechanism is a device with is able to transform power variables (torque, speed) in the way which is suitable for driving engine and also for required power parameters of the MWM. The gear mechanism is a combination of the gear components. The

input and output of gear mechanism is a shaft. The most frequently used gear components are gear wheels, mechanical clutches, pumps, motors, hydraulic torque converters and hydrodynamics clutches [14]. The gear mechanism functions are:

- Machine drive away.

- Change of machine travel direction.

- Interruption of power transfer (neutral gear),

- Braking with engine.

Hydrostatic transmission used in MWM allows continuous gear ratio change. Combination of HST and other gearing components increases rapidly gear ratio range in comparison with mechanical transmissions [14]. These features give hydrostatic transmission definitive advantage in the MWM technology.

Control system with equipment is essential part of each MWM powertrain. The control is such acting on the system, which provides demanded system behavior. The full automatization of MWM control is not possible because of non-recurring working cycle. The control of powertrain output variables: speed and torque is provided most frequently by combination of combustion engine and gear mechanism [14].

With current progress in electronics and application of mechatronics into MWM it is possible to increase quality and efficiency of complex system including control system which has great influence on MWM behavior.

3.4 Hydrostatic transmission (HST) of mobile working machine

Hydrostatic transmission of MWM is a mechanism, which uses pressure energy of fluid for energy transfer. The simplest configuration of HST consists of one pump and one motor with equipment. The advantage of HST is ability to change gear ratio continuously. This feature allows smooth motion and reduces number of mechanical gears [14].

The primary advantages of HST are continuous gear ratio change, simple transfer of big torque, high power density, simple reversing of drive and reliability. The primary disadvantages of HST powertrain are overall lower efficiency, higher price and dependence on parameters of used hydraulic oil.

The Figure 3.2 shows closed hydraulic circuit of HST produced by Sauer-Danfoss, concretely with bent axis variable displacement motor and swashplate variable displacement pump.

A description of oil circulation during forward MWM drive is following: The variable displacement motor converts mechanical energy to pressure energy. The hydraulic oil is transported from pump to motor thought high pressure loop of closed circuit. In the motor the pressure energy of oil is converted back to mechanical energy. The oil is transported

from motor to pump thought low pressure loop. This is a normal working cycle of HST.

The displacement change is provided by servo cylinder. The other parts of HST circuit are charge pump, oil reservoir, heat exchanger, relief valves and multi-functional valves . . .

This configuration allows four quadrant operations: two directions of rotating and two directions of driving/braking torque. The gear ratio change is realized by changing of pump or motor displacement. An Increase of the motor torque is possible with motor displacement increase. Increase of the motor speed by motor is possible with motor displacement decrease [10].

The reverse drive of MWM (equipped with HST) is realized by negative pump swash angle. The braking mode is based on the changed function of pump and motor. The maximal braking effect can be obtained by reverse mode setting. In this case the maximal braking effect is limited by setting of relief valve. The braking mode of HST reduces demands on the braking capabilities of diesel engine [14].
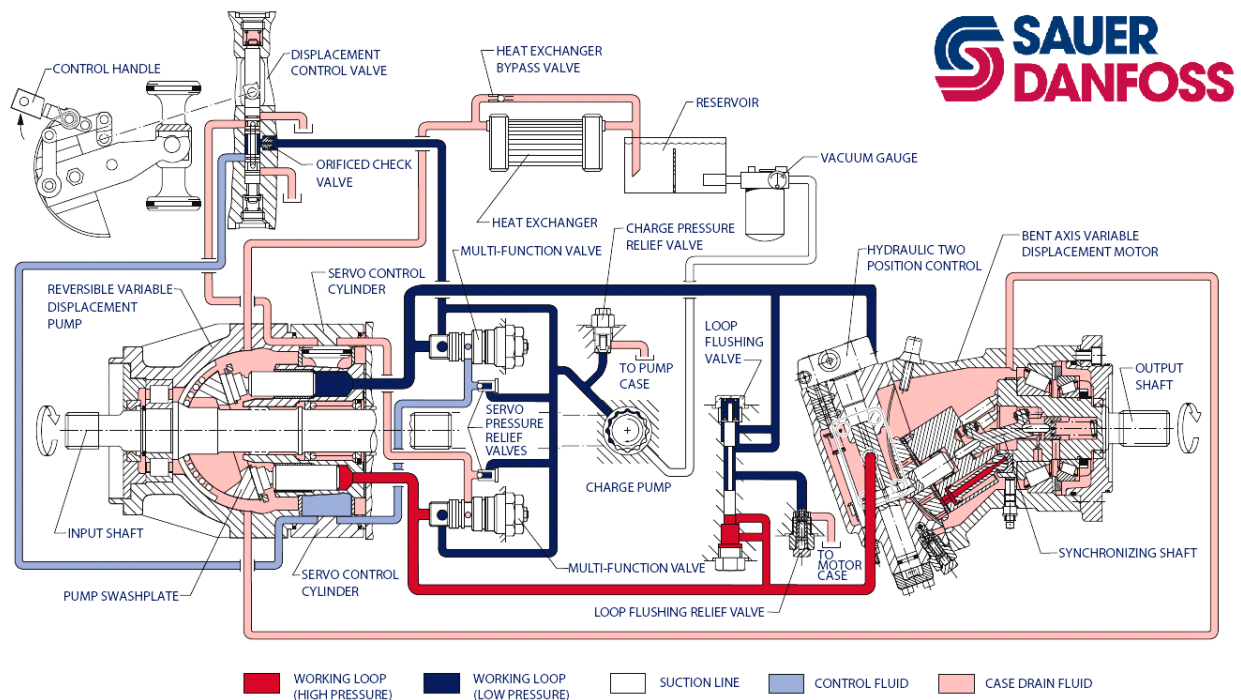
Figure 3.2: Sauer-Danfoss hydrostatic transmission [22]

3.5 Design of hydrostatic transmission powertrain

The basic design of hydrostatic transmission is based on the determination of working conditions, machine application and customer demands. The aim of HST powertrain design is optimalization of power and cost decreasing by suitable components selection. For calculation following data (common delivered by machine producer) are important:

- **Input parameters:**

  1. Machine type - application.
  2. Engine characteristics (power vs speed and torque vs speed).
  3. Vehicle mass m_{CoG} (loaded and unloaded).
  4. Wheel radius r_{w} (dynamic).

- **Demand output parameters:**

  1. Maximal tractive force F_{max}.
  2. Maximal vehicle speed v_{max}.
  3. Maximal grade ability δ.

The slope angle θ can be written as:

$$\theta = \arctan\left(\frac{\delta}{100}\right). \tag{3.1}$$

The total tractive force F_{w} required for vehicle movement (air resistance and acceleration resistance are neglected) is:

$$F_{\text{w}} = m_{\text{CoG}} \cdot 9.81 \cdot \Big(\sin(\theta) + \cos(\theta) \cdot f_{\text{r}} \Big), \tag{3.2}$$

where f_{r} is rolling resistance coefficient. In the case of heavy force F_{w}, it must be limited by adhesive conditions. The next step is detemination of corner (apparent) power:

$$P_{\text{C}} = F_{\text{w}} \cdot v_{\text{max}}. \tag{3.3}$$

The total gear ratio includes HST and mechanical transmission gear ratio. The gear ratio of complex gearing mechanism (R_{GM}) can be described by following equation:

$$R_{\text{GM}} = \frac{P_{\text{C}}}{P_{\text{max}} \cdot \eta_{\text{GB}} \cdot \eta_{\text{HST}}}, \tag{3.4}$$

where P_{max} is maximal engine power, η_{GB} is gearbox efficiency (normally 0.85-0.9) and η_{HST} is HST efficiency (normally 0.85). The HST gear ratio (R_{HST}) is described by following equations:

$$R_{\text{HST}} = \sqrt[z]{R_{\text{GM}}}, \tag{3.5}$$
$$R_{\text{HST}} = R^{\text{P}} \cdot R^{\text{M}}, \tag{3.6}$$

where Z is number of speed gears, R^{P} is pump gear ratio range and R^{M} is motor gear ratio range. The equation (3.6) gives presumption of pump and motor gear ratio combination in dependence on customer demands. However some rules existing for pump and motor selection. These rules are shown in Table 3.1.

HST gear ratio range	Pump	Motor
$R_{\mathrm{HST}} \leq 3.5$	Variable displacement pump	Constant motor
$R_{\mathrm{HST}} \leq 7$	Variable displacement pump	Swashplate motor
$R_{\mathrm{HST}} \leq 12$	Variable displacement pump	Bent axis motor

Table 3.1: Rules for motor and pump selection

Selection of pump and motor type is next step of motor frame selection. This selection is based on the corner motor power $P_{\mathrm{C}}^{\mathrm{M}}$ which can be obtained from:

$$P_{\mathrm{C}}^{\mathrm{M}} = R_{\mathrm{HST}} \cdot P_{\max}. \tag{3.7}$$

After determination of motor corner power and selection of correspondent motor size (with greater corner power than computed) is necessary to calculate motor maximal torque ($T_{\max}^{\mathrm{M}}$) and wheel maximal torque $T_{\max}^{\mathrm{W}}$:

$$T_{\max}^{\mathrm{M}} = \frac{V_{\max}^{\mathrm{M}} \cdot \Delta p \cdot \eta_{\mathrm{mh}}^{\mathrm{M}}}{2 \cdot \pi}, \tag{3.8}$$

$$T_{\max}^{\mathrm{W}} = m_{\mathrm{CoG}} \cdot 9.81 \cdot \mu_{\mathrm{L}} \cdot r_{\mathrm{w}}, \tag{3.9}$$

where $V_{\max}^{\mathrm{M}}$ is maximal motor displacement, Δp is pressure difference, $\eta_{\mathrm{mh}}^{\mathrm{M}}$ (0.93-0.98) is motor mechanical-hydraulic efficiency and μ_{L} is longitudinal friction coefficient. The mechanical (first) speed gear ratio i_1 can be obtained from:

$$i_1 = \frac{T^{\mathrm{W}}}{T_{\max}^{\mathrm{M}} \cdot \eta_{\mathrm{GB}}}. \tag{3.10}$$

The η_{GB} presents mechanical gearbox efficiency. The maximal motor speed $n_{\max}^{\mathrm{M}}$ can be obtained from:

$$n_{\max}^{\mathrm{M}} = \frac{v_{\max} \cdot i_2}{0.377 \cdot r_{\mathrm{w}}}, \tag{3.11}$$

where i_2 is second speed gear ratio. Speed gear ratios can be derived from demand maximal speed for each gear number. If the selection of motor is complete then following step is pump frame selection. Here is not easy situation as in motor frame selection. There are three possible ways for frame size ($V_{\max}^{\mathrm{P}}$) selection (only one and two speed gearboxes are used):

- Constant pump:

$$V_{\max}^{\mathrm{P}} = \frac{V_{\max}^{\mathrm{M}} \cdot n_{\max}^{\mathrm{M}}}{n_{\max}^{\mathrm{P}}} \cdot \frac{1}{\eta_{\mathrm{v}}^{\mathrm{P}}}, \tag{3.12}$$

- Variable displacement pump:

$$V_{\max}^{\mathrm{P}} = \frac{V_{\max}^{\mathrm{M}} \cdot n_{\max}^{\mathrm{M}}}{R^{\mathrm{M}} \cdot n_{\max}^{\mathrm{P}}} \cdot \frac{1}{\eta_{\mathrm{v}}^{\mathrm{P}}}, \tag{3.13}$$

21

- Variable displacement pump with two speed gearbox:

$$V_{\max}^{\mathrm{P}} = \frac{V_{\max}^{\mathrm{M}} \cdot n_{\max}^{\mathrm{M}}}{R^{\mathrm{M}} \cdot n_{\max}^{\mathrm{P}}} \cdot \frac{v_{\max}^{1}}{v_{\max}^{2}} \cdot \frac{1}{\eta_{\mathrm{v}}^{\mathrm{P}}}, \tag{3.14}$$

where $n_{\max}^{\mathrm{P}}$ is maximal pump (engine) speed, $\eta_{\mathrm{v}}^{\mathrm{P}}$ is volumetric pump efficiency, $v_{\max}^{1}$ is maximal vehicle first gear speed and $v_{\max}^{2}$ is maximal vehicle second gear speed. The last step of HST design is determination of minimal pump displacement ($V_{\min}^{\mathrm{P}}$) from equation

$$V_{\min}^{\mathrm{P}} = \frac{V_{\min}^{\mathrm{P}} \cdot n_{\max}^{\mathrm{P}}}{n_{\max}^{\mathrm{M}}} \cdot \eta_{\mathrm{v}}^{\mathrm{P}}. \tag{3.15}$$

The issue of HST powertrain design is very wide. Previous equations serve for approximated calculation. The final powertrain design is depending on the customer/producer demands and experiences. Equations in this Section (3.5) were taken from [14].

4 Model of mobile working machine in MATLAB-Simulink

The main purpose of the model of mobile working vehicle in MATLAB-Simulink is to test control algorithm of HST. Only few authors write about the dynamic modeling of complex MWM. Tinker developed detailed mathematical and physical powertrain model of wheel loader [24]. The dynamic models of powertrain are modeled in the thesis: Carter [6], Prasetiawan [17] and Zangh [30].

For dynamic modeling of MWM following literature can be used: references focused on car modeling: Vlk [26], Bauer [2], Kiencke and Nielsen [11], Rill [18]. Another useful reference is work written by Guzzella and Amstutz [8]. This work is focused on the fuel consumption of hybrid vehicles. Primary an object of all above mentioned references is not MWM, but these works deal with vehicles in general.

4.1 Powertrain model structure of mobile working machine

The Figure 4.2 shows one of possible powertrain structures of MWM. An each block - subsystem is equivalent to particular physical structure in the powertrain of MWM. A dividing of the powertrain into subsystems allows modular assembling of MWM powertrain in MATLAB-Simulink. The modular structure allows components configuration in dependence on the type of MWM. The selected powertrain structure is equivalent to powertrain structure used in telescopic loaders (manipulators). For example telehandler GTH - 5519 is shown in Figure 4.1.

Figure 4.1: Telehandler GTH$^{\text{TM}}$-5519 produced by GENIU [www.robinrents.com/]
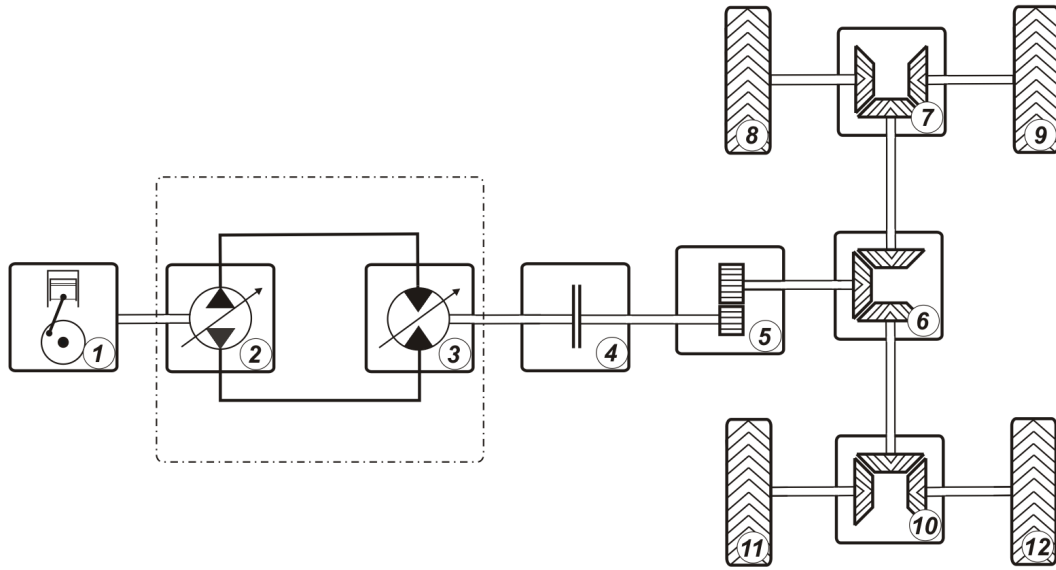
Figure 4.2: The selected powertrain structure of MWM: *1*-diesel engine, *2*-pump, *3*-motor, *4*-clutch, *5*-gearbox, *6*-central differential gear, *7*-front differential gear, *8*-front left wheel, *9*-front right wheel, *10*-rear differential gear, *11*-rear left wheel, *12*-rear right wheel.

4.2   Power transfer analysis of MWM powertrain

By modeling of MWM following variables must be determined:

- Variables or signals acting from environment to individual subsystems.
- Variables or signals acting from individual subsystems to environment.

The mechatronic systems operate with kinematic and power variables. The variables velocity and force (angular velocity and torque) are important for MWM powertrain simulation. The variables flow and pressure are important for HST analyzing.

The reciprocal action of kinematic and power variables in MWM powertrain is shown in Figure 4.3. The variables and signals present input and output data coming to and from individual model subsystems. The direction of vehicle movement is defined by the sign of wheel's speed. The positive value of speed belongs to vehicle forward drive. The negative value of speed belongs to vehicle reverse drive. Analogous to the motoring mode (for example during vehicle acceleration the energy is transferred from engine to wheel) the value of the wheel's output torque is positive. During braking mode (for example during downhill drive the energy is transferred from wheel to engine) the value of the wheel's torque is negative.

In the case of MWM flat (2D) model the powertrain consists of front and rear axle (wheel), central differential gear (transfer gear), gearbox, hydrostatic transmission and diesel engine.
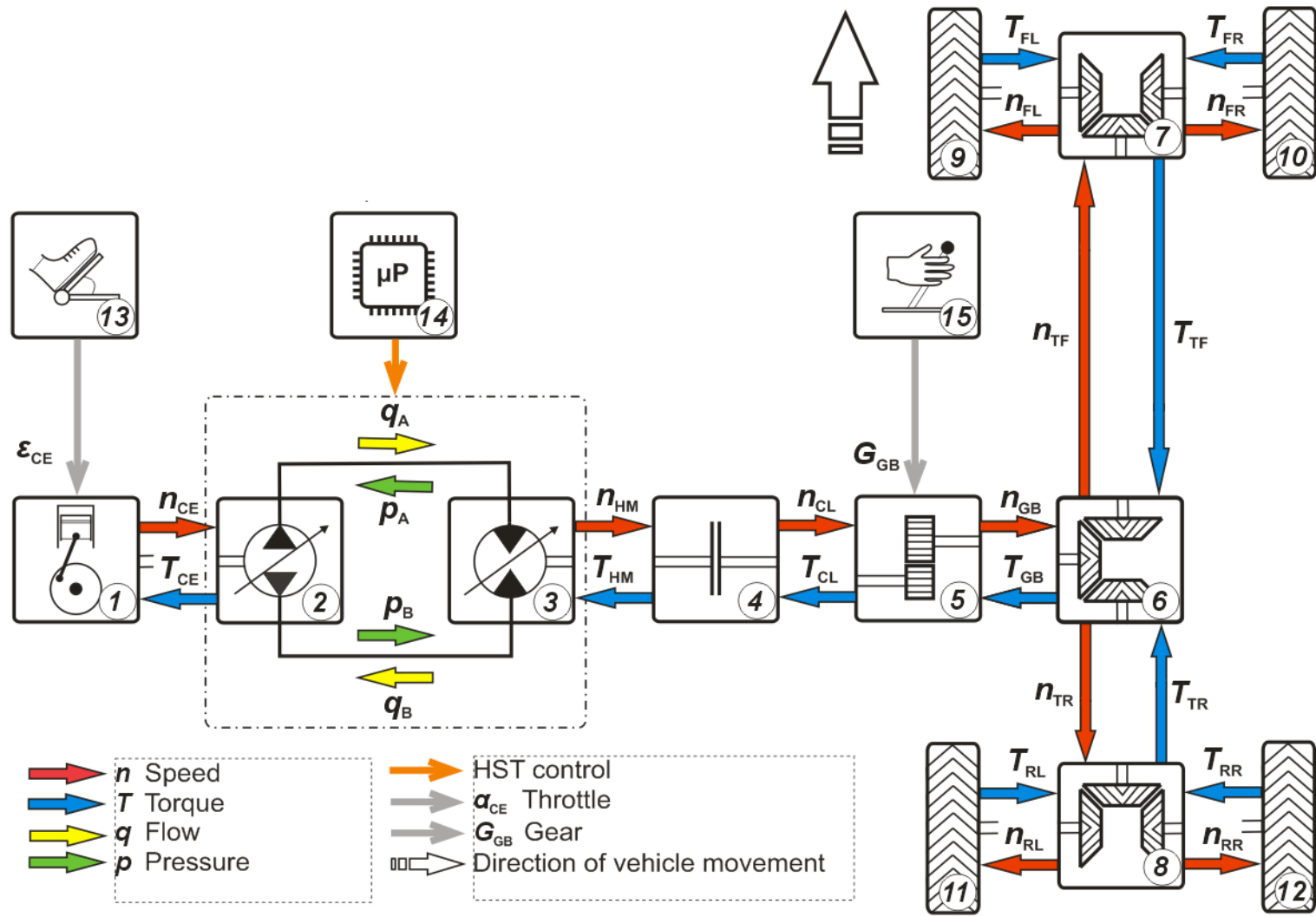
Figure 4.3: Powertrain structure of MWM with kinematic and power variables direction : *1*-diesel engine, *2*-pump, *3*-motor (Connection of pump and motor presented HST), *4*-clutch, *5*-gearbox, *6*-central differential gear, *7*-front differential gear, *8*-front left wheel, *9*-front right wheel, *10*-rear differential gear, *11*-rear left wheel, *12*-rear right wheel, *13*-accelerator (throttle) pedal, *14*-HST control, *15*-shift control

4.3   Diesel engine model

Mathematical and physical modeling of diesel engine (in Figure 4.3 number *1*) is extensive task. The developed models differ and depend on the model application. The models of engine control unit are usually very detailed. The engine models for complex system simulation are less detailed. The most of the engine models are based on the measured characteristics.

The modeling of turbocharged diesel engine is more complicated then modeling of petrol engine because the diesel engine design is more complex. Relatively accurate and detailed model was developed by Yanakiev and Kannellakopoulos [28]. This model is a base for another works. Comparatively detailed model was modeled by Strandh [23]. The author stated that the created petrol engine is more stable then diesel engine model. Another works were developed by Biteus [4] and Zackrisson [29]. The theory of combustion engines (CE) is analyzed by Kiencke and Nielsen [11]. A necessity of measured characteristics is prime disadvantage of the previous works.

Simpler models were developed by Tinker [24] and Donald [7]. Donald modeled complex powertrain model of racing vehicle only with petrol engine. A useful work was created by Zackrisson [29] in Dymola language. The combustion engines were also modeled by [18] Rill and Mussaeus [16].

For purposes of modeling related to MWM powertrain it is required to develop simple and fast model. Also in reality it is difficult to get the engine characteristics and parameters. For this reason the created model has to use minimum of measured characteristics even by decreasing accuracy. The modeling of diesel engine is based on the Newton's second law of motion:

$$J_{\mathrm{CE}}\dot{\omega}_{\mathrm{CE}} = T_{\mathrm{ID}} - T_{\mathrm{CE}}, \tag{4.1}$$

where the engine's moment of inertia J_{CE} is considered as a constant, ω_{CE} (n_{CE}) is engine speed.

The indicated shaft torque T_{ID} can be calculated as

$$T_{\mathrm{ID}} = T_{\mathrm{CO}} - T_{\mathrm{FE}}, \tag{4.2}$$

where T_{CO} is a combustion torque and T_{FE} is a friction torque (which cause friction losses in engine).

The indicated torque T_{ID} can be also written as

$$T_{\mathrm{ID}} = f(n_{\mathrm{CE}}, fr_{\mathrm{CE}}), \tag{4.3}$$

where fr_{CE} is relative fuel rack position.

An operating of diesel engine by driver requires a usage of controller. The diesel engines are equipped with power or speed regulators. The most frequently used is the speed controller. The demand of engine speed is set by position of accelerator pedal (fuel rack). For this purpose a simple proportional speed regulator is used [14]. Nowadays there

are more advanced control algorithms, which are implemented in the diesel engines. For example RQV control (RQV is a description of the German *"Regler Menge Vestell"*), more information about RQV are in [11] and [29].

The Equations (4.4) ... (4.6) describing applied speed proportional regulator:

$$fr_{\mathrm{CE}} = K_{\mathrm{CE}} \cdot e_{\mathrm{CE}}, \tag{4.4}$$

$$e_{\mathrm{CE}} = n_{\mathrm{CE}} - n_{\mathrm{DE}}, \tag{4.5}$$

$$n_{\mathrm{DE}} = (n_{\max} - n_{\mathrm{idl}}) \cdot \varepsilon_{\mathrm{CE}} \cdot 0.01 + n_{\mathrm{idl}}, \tag{4.6}$$

where K_{CE} is a gain of regulator proportional, $\varepsilon_{\mathrm{CE}}$ is a position of accelerator pedal. The maximal engine speed is $n_{\max}$, the idling engine speed is n_{idl}. The speed control deviation is e_{CE} and n_{DE} is demanded engine speed.

The engine dynamic (pistons, piston rods, crankshaft) is modeled in Equation (4.1). The dynamic of fuel injection is not included in this equation. If the dynamic of injection (fuel transport delay) is not included in the model then the model results are unrealistic. For injection dynamic simulation can be simple used transfer function. The primary problem of transfer function is estimation of function parameters. Tinker [24] modeled fuel transport delay by a following equation:

$$\frac{\mathrm{d}}{\mathrm{d}t} fr_{\mathrm{CE}} = \frac{fr_{\mathrm{PD}} - fr_{\mathrm{CE}}}{t_{\mathrm{fr}}}, \tag{4.7}$$

where fr_{PD} represents actual fuel rack position in consideration of accelerator pedal position. t_{fr} is fuel transport delay. Both methods (transfer function and fuel delay) were approved. The last model version uses fuel transport delay.

A speed regulator (RQV) [29] defines exact values of proportional gain. If the modeled engine has the similar parameters as engine in [29] than characteristics from [29] can be used in the model. These characteristics were implemented in the diesel engine model. The modeled RQV regulator is based on the following equation:

$$K_{\mathrm{CE}} = \begin{cases} 0, & \text{for } n_{\mathrm{DE}} < n_{\mathrm{CE}}, \\ 1, & \text{for } e_{\mathrm{CE}} > e_{\mathrm{alw}}, \\ \frac{e_{\mathrm{CE}}}{e_{\mathrm{alw}}}, & otherwise, \end{cases} \tag{4.8}$$

where e_{alw} is parameter determined from injected fuel, actual accelerator pedal position and speed deviation e_{CE}. The resulting e_{alw}-map is shown in Figure 4.4 [29].

The developed model is prepared to engine braking mode where: $T_{\mathrm{CO}} < T_{\mathrm{FE}}$. Than the indicated torque T_{ID} is negative and vehicle brakes. The engine's braking mode is controlled by control unit. The braking torque (during maximal engine braking effect) with neglected temperature effect can be written as

$$T_{\mathrm{ID}} = f(n_{\mathrm{CE}}). \tag{4.9}$$

The braking torque can be considered as linear as shown in Figure 4.5 [29]. The shuffle (braking) torque map is estimated only from [14].
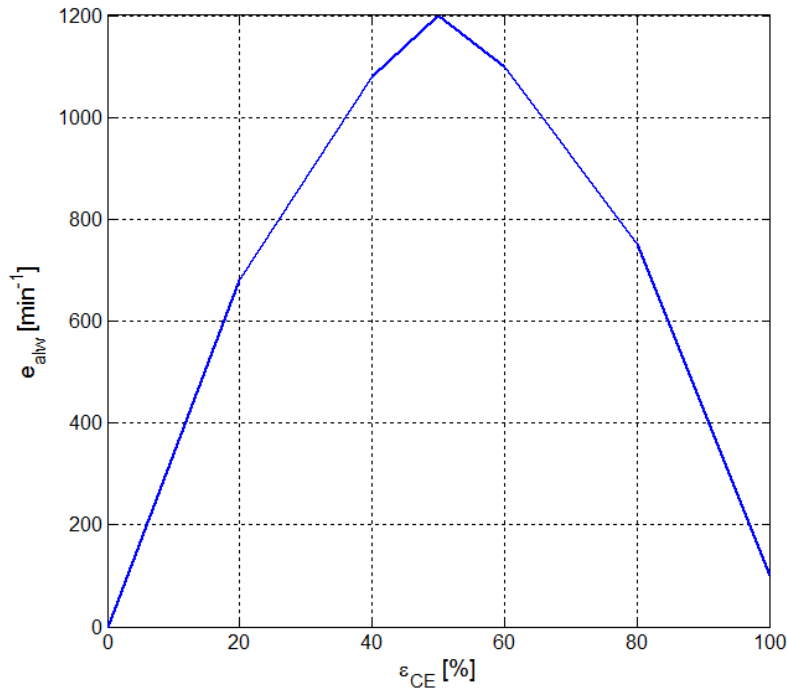
Figure 4.4: Allowed speed difference

One of the most important requirements is modeling (estimating) of MWM fuel consumption. The most of the models use measured characteristics. The fuel consumption g_{CE} can be written as a function: $g_{CE} = f(n_{CE}, T_{ID})$. The fuel consumption can be simple estimated from this map as shown in figure 4.6 [13].

Diesel engine model is based on the previous equations. The equations inputs and outputs of these equations were modified according to diesel engine block as shown in Figure 4.3. The inputs and outputs in the MATLAB-Simulink (shown in Table 4.1) must be compatible with other Simulink blocks (subsystems). The diesel engine in Simulink is illustrated in Figure A.1.

Diesel engine block allows simple setting of tunable parameters in subsystem mask shown in Figure 4.7. User can simply set up: maximal engine power, minimal engine speed, maximal engine speed, idling engine speed, minimal fuel consumption, fuel transport delay, engine's moment of inertia and shuffle torque.
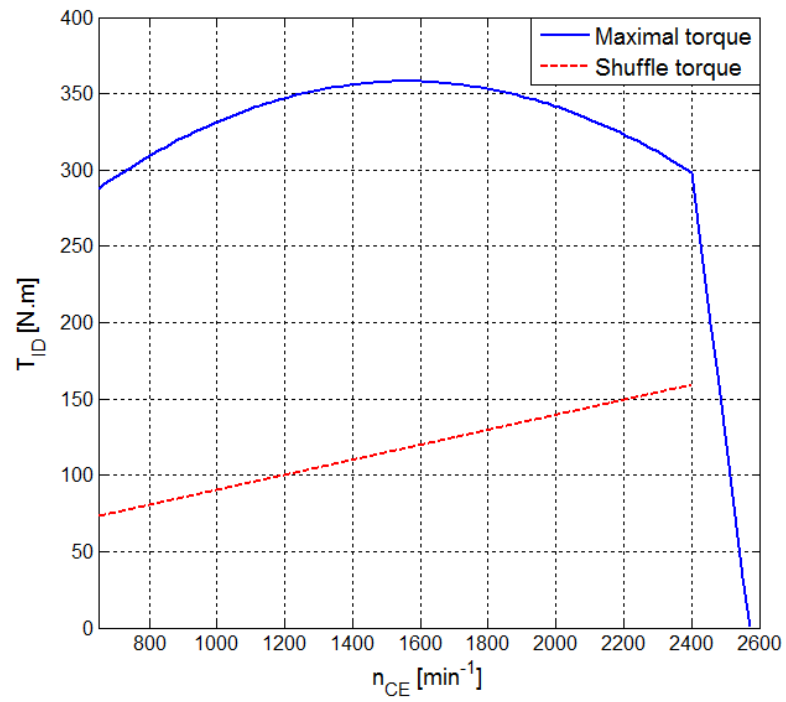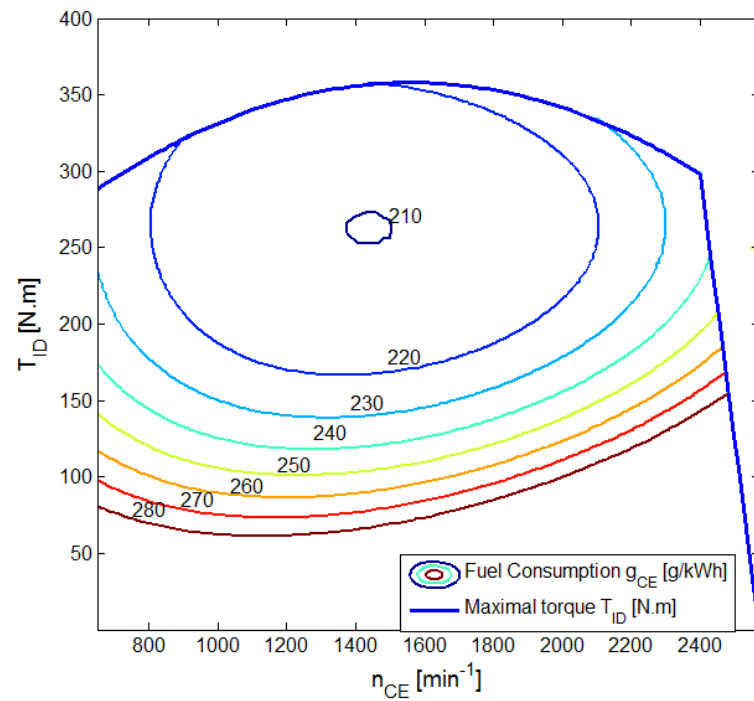
Figure 4.5: Maximal and shuffle engine torque

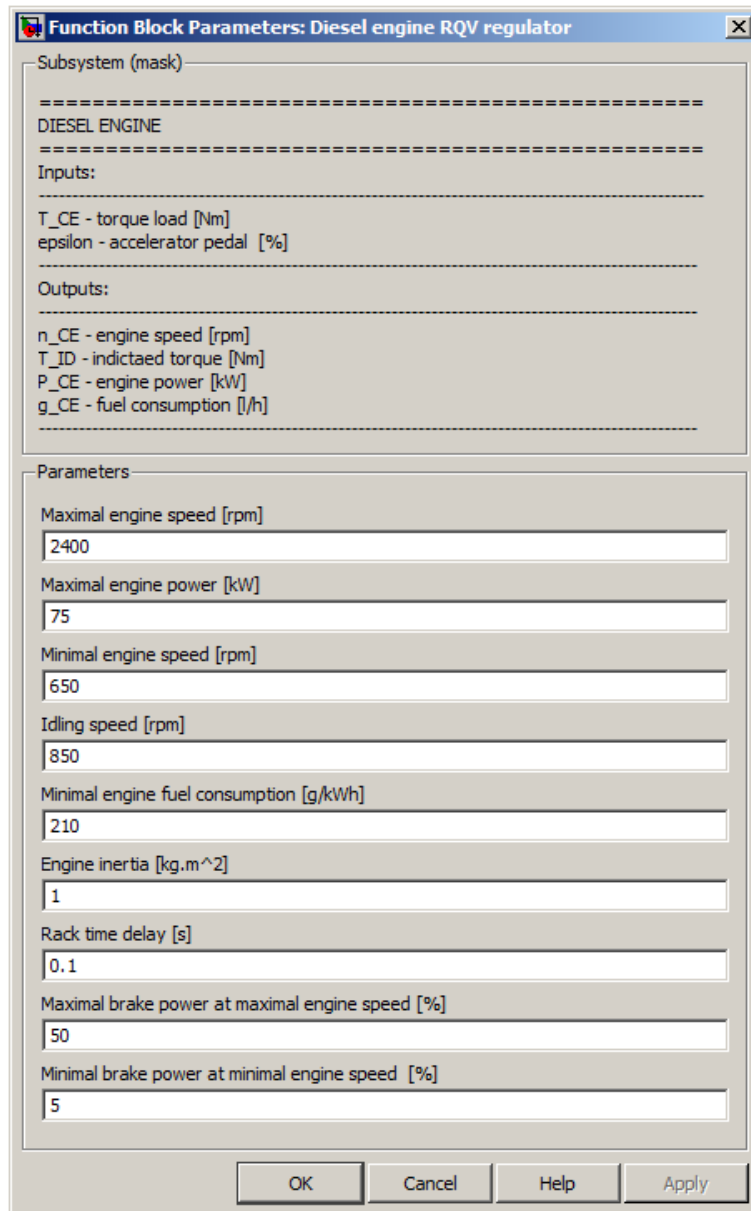Figure 4.6: Fuel consumption map

Figure 4.7: Diesel subsystem mask

DIESEL ENGINE			
Signal	Description	Symbol	Unit
INPUTS	Load torque from HG	T_{CE}	N·m
	Accelerator pedal position	$\varepsilon_{\mathrm{CE}}$	%
OUTPUTS	Engine speed	n_{CE}	min^{-1}
	Engine power	P_{CE}	kW
	Indicated torque	T_{ID}	N·m
	Fuel consumption	g_{CE}	$\mathrm{l\cdot h}^{-1}$

Table 4.1: Diesel engine inputs and outputs[1]

4.4 Hydrostatic transmission model

The hydrostatic transmission model is based on the modeling of pump and motor. Other important components of HST are charge pump, hoses, valves and control components. A difficulty and size of the HST model depends on the detail level.

Carlosson developed very good HST model in a forest vehicle [5]. A hydrostatic transmission focused on control was modeled by Carter [6], Prasetiawan [17] and Zhang [30]. The basic mathematical description of pump (4.10) ... (4.13) and motor (4.14) ... (4.17) results in the following equations:

$$\zeta^{\mathrm{P}} \quad = \quad \frac{\tan \tau}{\tan \tau_{max}}, \tag{4.10}$$

$$T^{\mathrm{P}} \quad = \quad \frac{\Delta p . V_{\max}^{\mathrm{P}} . \zeta^{\mathrm{P}}}{2.\pi.\eta_{\mathrm{mh}}^{\mathrm{P}}}, \tag{4.11}$$

$$n^{\mathrm{P}} \quad = \quad \frac{Q^{\mathrm{P}}}{V_{\max}^{\mathrm{P}} . \zeta^{\mathrm{P}} . \eta_{\mathrm{v}}^{\mathrm{P}}} \cdot 60, \tag{4.12}$$

$$\eta^{\mathrm{P}} \quad = \quad \frac{P_{\mathrm{h}}^{\mathrm{P}}}{P_{\mathrm{m}}^{\mathrm{P}}} = \frac{Q^{\mathrm{P}}.\Delta p}{2\pi.T^{\mathrm{P}}.n^{\mathrm{P}}} = \eta_{\mathrm{v}}^{\mathrm{P}}.\eta_{\mathrm{mh}}^{\mathrm{P}}, \tag{4.13}$$

$$\zeta_{\mathrm{M}} \quad = \quad \frac{\sin \tau}{\sin \tau_{max}}, \tag{4.14}$$

$$T^{\mathrm{M}} \quad = \quad \frac{\Delta p . V_{\max}^{\mathrm{M}} . \zeta^{\mathrm{M}} . \eta_{\mathrm{mh}}^{\mathrm{M}}}{2.\pi}, \tag{4.15}$$

$$n^{\mathrm{M}} \quad = \quad \frac{Q^{\mathrm{M}} . \eta_{\mathrm{v}}^{\mathrm{M}}}{V_{\max}^{\mathrm{M}} . \zeta^{\mathrm{M}}} \cdot 60, \tag{4.16}$$

$$\eta^{\mathrm{M}} \quad = \quad = \frac{P_{\mathrm{h}}^{\mathrm{M}}}{P_{\mathrm{m}}^{\mathrm{M}}} = \frac{Q_{\mathrm{M}} . \Delta p}{2\pi.T^{\mathrm{M}}.n^{\mathrm{M}}} = \eta_{\mathrm{v}}^{\mathrm{M}}.\eta_{\mathrm{mh}}^{\mathrm{M}}, \tag{4.17}$$

where ζ^{P} is regulation parameter, τ is swash plate or bent axis angle, T^{P} is pump torque (for selected configuration $T^{\mathrm{P}} = T_{\mathrm{CE}}$), Δp is pressure difference, $V_{\max}^{\mathrm{P}}$ is maximal pump

---

[1]Green color match with Simulink inputs and magenta color match with Simulink outputs.

displacement, n^P is pump speed (for selected configuration $n^P = n_{CE}$), Q^P is pump flow, η_v^P is pump volume efficiency, η_{mh}^P is mechanical-hydraulic efficiency, P_h^P is pump hydraulic power and P_m^P is pump mechanical power. Signs are analogical valid also for motor.

A determination of HST efficiency is a serious problem for HST modeling. A total efficiency is not constant and also it is not a function of one or two variables. The Sauer-Danfoss pump/motor model uses function for efficiency determination based on measured data. For this reason the Sauer-Danfoss model has a very good correspondence between simulated and measured efficiencies.

Sauer-Danfoss swashplate pump and bent axis motor were selected for Telehandler application. Particularly motor S51 with maximal displacement 110 cm³ and pump H1 with maximal displacement 78 cm³ as shown in Figure 4.8. H1ump is axial piston pump with swash plate design. S51 motor is axial piston motor with bent axis design. The application of variable displacement pump/motor (primary and secondary regulation) allows decreasing of fuel consumption. The HST model is shown in Figure A.2. The model inputs and outputs in Simulink are represented in Table 4.2. In the final model user has no access to model's inside, because HST model was delivered in s-function form.

HYDROSTATIC TRANSMISSION			
Signal	Description	Symbol	Unit
INPUTS	Speed from engine	n_{CE}	min⁻¹
	Speed from clutch	n_{HM}	min⁻¹
	Demand pump angle	P_{angle}	%
	Demand motor angle	M_{angle}	%
OUTPUTS	Load torque to CE	T_{CE}	N·m
	Load torque to clutch	T_{HM}	N·m

Table 4.2: Hydrostatic transmission inputs and outputs[2]

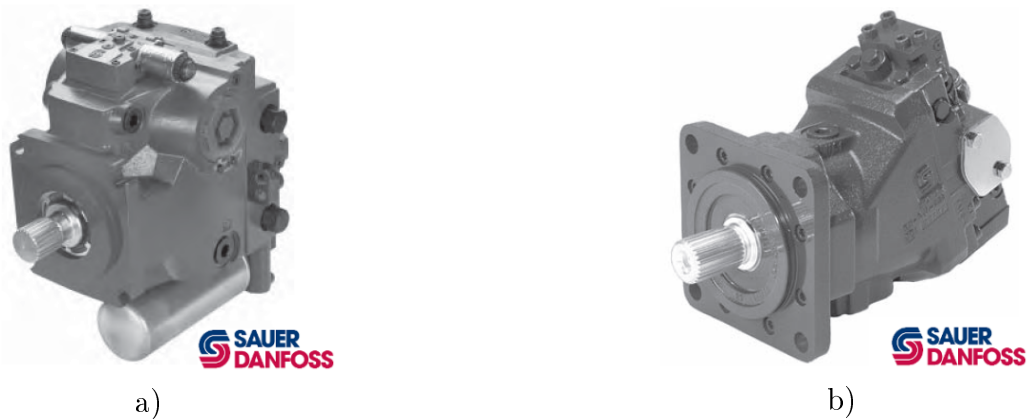
a)   b)

Figure 4.8: a)–Sauer-Danfoss H1 pump, b)–Sauer-Danfoss S51 motor [9], [22]

[2]Green color match with Simulink inputs and magenta color match with Simulink outputs.

4.5   Gearbox and clutch model

The gearbox model (in Figure 4.3 number *5*) can be developed by different methods. The first method is based on excellent knowledge of gearbox design. This way was used by Beckers [3] during hybrid drive modeling. For selected telehandler application the second method is more suitable. It is based on the parameters obtained from producer catalogues or measurements. The correct dynamic gearbox model requires knowledge of the following parameters: gear ratio of speed gears, gearbox moment of inertia, gearbox stiffness and gearbox damping. A determination of these parameters is very difficult. This second method was used by Tinker [24] and Donald [7].

With respect to powertrain concept, a clutch (which is commonly included in automatic gearbox) does not need individual model. The clutch modeling is very difficult and inaccurate, because the clutch parameters are not available. If the clutch model is not included by gear shift modeling than this fact must be considered by evaluation of results.

A simpler gearbox model, which does not use unknown stiffness and damping parameters is required. Then this model is more static. It is sufficient for steady states simulation and states, where the dynamic of gearbox is not important. This model type was modeled by Guzzela [8] and by Mussaeus [16].

The basic gearbox equations are [8]:

$$T_{\mathrm{CL}} = \frac{T_{\mathrm{GB}}}{i_{\mathrm{GB}} \cdot \eta_{\mathrm{GB}}}, \tag{4.18}$$

$$T_{\mathrm{CL}} = \frac{T_{\mathrm{GB}}}{i_{\mathrm{GB}}} \cdot \eta_{\mathrm{GB}}, \tag{4.19}$$

$$\omega_{\mathrm{CL}} = \omega_{\mathrm{CL}} \cdot i_{\mathrm{GB}}, \tag{4.20}$$

where T_{CL} is torque acting from clutch to gearbox, T_{GB} is torque acting from gearbox to central differential gear. If the model of clutch is neglected then $T_{\mathrm{CL}} = T_{\mathrm{HM}}$ and $n_{\mathrm{CL}} = n_{\mathrm{HM}}$. The i_{GB} presents actual gear ratio and η_{GB} presents gearbox efficiency. The gearbox efficiency is the same for driving and braking mode.

The Equation (4.18) is valid for normal drive mode (vehicle is driving with the engine) and the Equation (4.19) is valid for braking mode (vehicle is braking with the engine). The control input G_{GB} represents actual speed gear.

The equation's inputs and outputs were modified. The inputs and outputs in the MATLAB-Simulink (shown in Table 4.3) must be compatible with other Simulink blocks (subsystems). In the last Simulink model version an influence of gearbox inertia (shown in Figure A.3) is implemented. The influence of gearbox inertia is modeled only by approximation of numerical derivation. However the real influence of this inertia on gearbox dynamics must be considered carefully.

The gearbox block allows simple setting of tunable parameters in the subsystem mask. User can simple set up: gearbox efficiency, gear ratios and other parameters,of which using must be further detail tested in the future (for example inertia approximation ...). All unverified parameters and setting are initially set to zero.

GEARBOX			
Signal	Description	Symbol	Unit
INPUTS	Speed from transfer case	n_{GB}	min^{-1}
	Torque from clutch	T_{CL}	N·m
	Actual speed gear	G_{GB}	-
OUTPUTS	Speed to clutch	n_{CL}	min^{-1}
	Load torque to central differential gear	T_{GB}	N·m

Table 4.3: Gearbox inputs and outputs[3]

4.6 Central differential gear model

A central differential gear (in Figure 4.3 number 5) redistributes power between front and rear vehicle axle. More information about central differential gears was written by Vlk [27] and Rill [19]. Basic information about central differential gear is also described by Bauer [2] and Tinker [24]. There are many types of central differential gears nowadays exist and the central differential gears issue is relatively complex. The developed model is modeled as a common central differential gear (without friction effect, Haldex or Torsen clutch...). This model operates only in the locked and open mode.

The differential gear function is eliminated in the locked mode. In this case the differential gear serves as a simple transfer case. The transfer case is used in tractors [2], when the gear ratio between front and rear axle is constant. The second case is open mode. The open differential mode is more convenient for implementation in Simulink. In this case (open mode) the central differential gear fully performs its function. If the differential gear efficiency and gear inertia are neglected and if gear ratio equals one then following equations can be written:

$$T_{\mathrm{GB}} \cdot n_{\mathrm{GB}} = T_{\mathrm{TF}} \cdot n_{\mathrm{TF}} + T_{\mathrm{TR}} \cdot n_{\mathrm{TR}}, \tag{4.21}$$

$$T_{\mathrm{TF}} = \frac{T_{\mathrm{GB}} \cdot n_{\mathrm{GB}}}{i_{\mathrm{T}} \cdot n_{\mathrm{TR}} + n_{\mathrm{TF}}}, \tag{4.22}$$

$$T_{\mathrm{GB}} = T_{\mathrm{TF}} + T_{\mathrm{TR}}, \tag{4.23}$$

$$i_{\mathrm{T}} = \frac{T_{\mathrm{TR}}}{T_{\mathrm{TF}}}, \tag{4.24}$$

$$n_{\mathrm{GB}} = n_{\mathrm{TF}} = n_{\mathrm{TR}}. \tag{4.25}$$

The Equations (4.21) and (4.22) are based on the energy conversion law, which is valid for differential gears in general. The locked differential gear is described by Equations (4.23), (4.24) and (4.25). i_T presents actual torque ratio between front and rear axle (the other labels are corresponding with Figure 4.3). Generally the i_T does not equal to one and then the central differential gear is not symmetrical. For open central differential gear following can be derived:

---

[3]Green color match with Simulink inputs and magenta color match with Simulink outputs.

$$n_{\text{GB}} = \frac{n_{\text{TF}} + n_{\text{TR}}}{2}, \qquad (4.26)$$

$$T_{\text{GB}} = T_{\text{TF}} + T_{\text{TR}}, \qquad (4.27)$$

$$i_{\text{T}} = \frac{T_{\text{TR}}}{T_{\text{TF}}}. \qquad (4.28)$$

The Equation (4.28) is the same as Equation (4.24). The difference is in the open mode when i_{T} is constant and in the locked mode when i_{T} is a variable depending on the actual axles coefficients of traction.

A combination of the previous equations and equations from Chapter 4.5 (concretely Equations (4.18) and (4.19)) allows modeling of open central differential gear in Simulink. The locked differential gear is only approximated in regard of vehicle concept. The locked mode approximation uses proportional torque regulator, which redistributes drive torque between front and rear axle in such a way that the front and rear axle speed is the same. The model implementation in the MATLAB-Simulink is shown in Figure A.4. The inputs an outputs in Simulink (shown in Table 4.4) must be compatible with other Simulink blocks (subsystems).

The model block of central differential gear allows simple setting of tunable parameters in subsystem mask. User can simply set up: gear efficiency, gear ratio (final gear ratio), torque distribution ratio and other parameters or subsystems which using must be further tested in the future (for example inertia approximation, differential gear locking ...). All unverified parameters and setting are initially set to zero.

CENTRAL DIFFERENTIAL GEAR			
Signal	Description	Symbol	Unit
INPUTS	Speed from front differential gear/axle	n_{TF}	min^{-1}
	Speed from rear differential gear/axle	n_{TR}	min^{-1}
	Load torque from gearbox	T_{GB}	N·m
OUTPUTS	Load torque to front differential gear/axle	T_{TF}	N·m
	Load torque to rear differential gear/axle	T_{TR}	N·m
	Speed to gearbox	n_{GB}	min^{-1}

Table 4.4: Central differential gear inputs and outputs[4]

4.7 Wheel model

Nowadays a wheel and tire modeling is one of the most complicated issues in the vehicle simulations. The basic problem is exact determination of traction forces. For this reason the wheel and tire modeling is the most difficult part from powertrain modeling.

---

[4]Green color match with Simulink inputs and magenta color match with Simulink outputs.
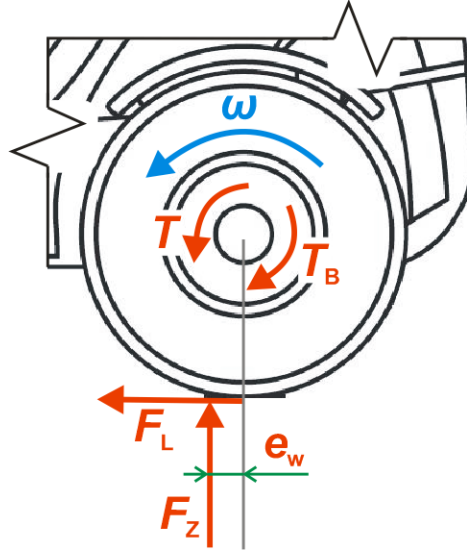
Figure 4.9: Forces acting on a wheel

The wheel in Figure 4.3 is illustrated by blocks number *9, 10, 11* and *12*. A determination of tractive forces is necessary for vehicle's speed computing. The Figure 4.9 shows the forces acting on a vehicle. From this figure following equation can be obtained [26]:

$$J_{\mathrm{w}} \frac{d\dot{\omega}_{\mathrm{w}}}{dt} = T_{\mathrm{T}} - T_{\mathrm{B}} - F_{\mathrm{L}} \cdot r_{\mathrm{w}} - F_{\mathrm{Z}} \cdot f_{\mathrm{r}}, \tag{4.29}$$

where T_{T} is the driving torque of a wheel, T_{B} is the braking torque, F_{L} is a tractive longitudinal force. The wheel load F_{Z} is normal force acting on the wheel/axle. J_{w} is a wheel moment of inertia. The ω_{w} is wheel speed, the r_{w} is wheel radius. The rolling resistance coefficient is obtained from:

$$f_{\mathrm{r}} = \frac{e_{\mathrm{w}}}{r_{\mathrm{w}}}, \tag{4.30}$$

where e_{w} is a radius of rolling resistance. The f_{r} parameters for various surfaces are shown in Table 4.5 [26].

If the wheel spin is assumed then the Equation (4.29) contains two unknown variables: F_{L} and $\dot{\omega}_{\mathrm{w}}$. The traction force F_{L} determination is complicated and the majority of developed models use empirical knowledge. The Pacejka magix formula [1] and Burckhadt model [11] are mostly used in vehicle simulations. For selected application the Burckhadt model is chosen.It is simpler for longitudinal wheel slip alone. The Burckhadt model of wheel slip is described by equations:

$$\mu_{\mathrm{L}} = \frac{F_{\mathrm{L}}}{F_{\mathrm{Z}}}, \tag{4.31}$$

$$\mu_{\mathrm{L}} = c_1 \cdot (1 - e^{-c_2 \cdot s_{\mathrm{L}}}) - c_3 \cdot s_{\mathrm{L}}, \tag{4.32}$$

where μ_L is a longitudinal friction coefficient. The parameters c_1, c_2 and c_3 are empirical parameters various for different surfaces obtained from Table 4.6 [11]. The s_L is a longitudinal wheel slip. The longitudinal friction coefficient as a function of longitudinal slip is shown in Figure 4.10.

Surface	f_r [-]	Surface	f_r [-]
Asphalt	0.01-0.02	Grass	0.08-0.15
Concrete	0.015-0.025	Sand	0.15-0.30
Cobblestone	0.02-0.03	Snow	0.20-0.30
Field path - dry	0.04-0.15	Mud	0.20-0.40
Field path - wet	0.08-0.20	Ice	0.01-0.025

Table 4.5: Parameter sets for rolling co-efficients [26]

Surface/parameter	c_1 [-]	c_2 [-]	c_3 [-]
Asphalt, dry	1.2801	23.99	0.52
Asphalt, wet	0.857	33.822	0.347
Concrete, dry	1.1973	25.168	0.5373
Cobblestones, dry	1.3713	6.4565	0.6691
Cobblestones, wet	0.4004	33.7080	0.1204
Snow	0.1946	94.129	0.0646
Ice	0.05	306.39	0

Table 4.6: Parameter sets for friction coefficient characteristics-Burckhardt [11]

The wheel slip s_L can be written as [11]:

$$s_L = \frac{\omega_w \cdot r_w - v_{CoG}}{v_{CoG}}, \tag{4.33}$$

$$s_L = \frac{\omega_w \cdot r_w - v_{CoG}}{\omega_w \cdot r_w}, \tag{4.34}$$

$$s_L = \frac{-(v_{CoG} - r_w \cdot \omega_w)}{r_w \cdot |\omega_w|}. \tag{4.35}$$

During vehicle driving $\omega_w \cdot r_w > v_{CoG}$ Equation (4.34) is valid, during vehicle braking $\omega_w \cdot r_w \leq v_{CoG}$ Equation (4.33) is valid. The Rill [18] derived wheel slip in Equation (4.35).

The block model in the MATLAB-Simulink (shown in Figure A.5) was developed by implementation of previous equations. The inputs and outputs in Simulink (shown in Table 4.7) must be compatible with other Simulink blocks (subsystems). The developed wheel block allows simple setting of tunable parameters in subsystem mask shown in Figure 4.11. The user can simply set up: wheel surface type, rolling resistance coefficient, wheel radius and wheel moment of inertia.
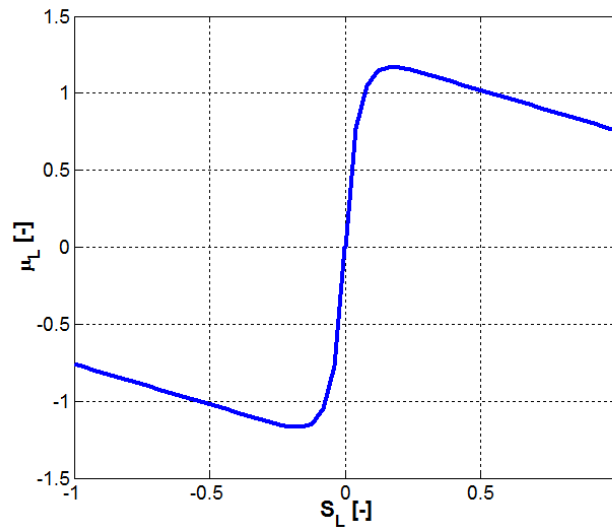
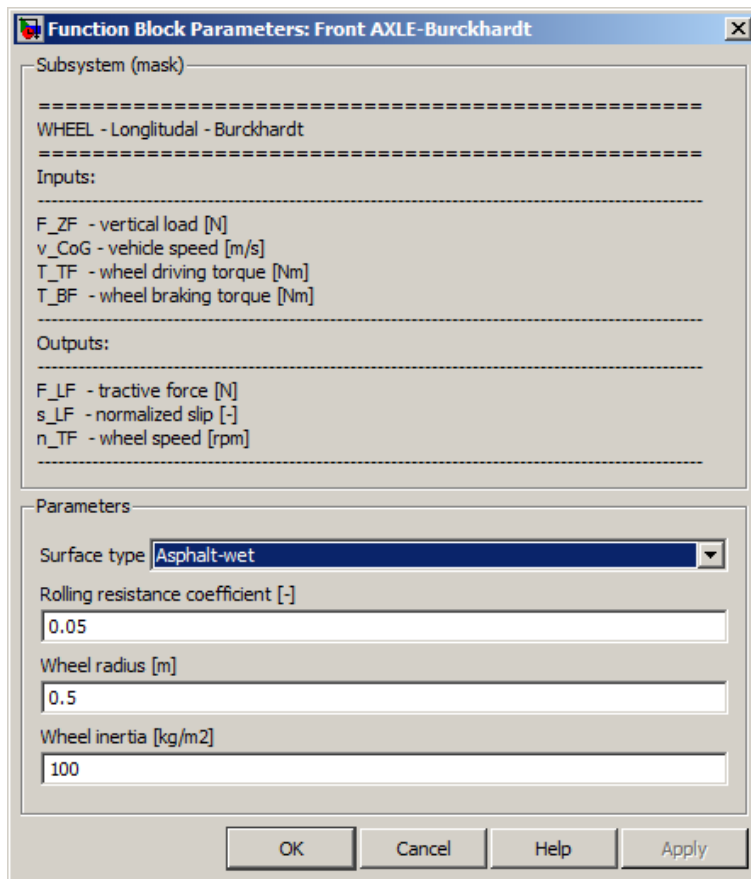Figure 4.10: The longitudinal friction coefficient μ_L as a function of longitudinal wheel slip s_L (for asphalt dry)

Figure 4.11: Wheel subsystem mask

FRONT WHEEL (AXLE)			
Signal	Description	Symbol	Unit
INPUTS	Load torque from transfer case	T_{TF}	N·m
	Braking torque	T_{BF}	N·m
	Tire normal load	F_{ZF}	N
	Vehicle (CoG) speed	v_{CoG}	m·s^{-1}
OUTPUTS	Wheel (axle) speed	n_{TF}	min^{-1}
	Wheel (axle) longitudinal slip	s_{LF}	-
	Wheel (axle) longitudinal force	F_{LF}	N

Table 4.7: Wheel model inputs and outputs - forward drive[5]

4.8 Vehicle body model

The vehicle dynamic is mainly analyzed by Vlk [26], Nielsen, Kiencke [11] and Rill [18]. Very good models were developed by other authors too.

A simple 2D model (shown in Figure 4.12) is used for creating of vehicle dynamic model. This model has 3 degrees of freedom and expects only forward or reverse vehicle drive. The developed model is based on the following equations :

$$m_{\text{CoG}} \cdot \dot{v}_{\text{CoG}} = F_{\text{LF}} + F_{\text{LR}} - m_{\text{CoG}} \cdot g \cdot \sin\theta - F_{\text{AR}}, \tag{4.36}$$

$$0 = F_{\text{ZF}} + F_{\text{ZR}} - m_{\text{CoG}} \cdot g \cdot \cos\theta, \tag{4.37}$$

$$0 = F_{\text{ZF}} \cdot (l_{\text{F}} + l_{\text{R}}) + (F_{\text{AR}} + m_{\text{CoG}} \cdot g \cdot \sin\theta + m \cdot \dot{v}_{\text{CoG}}) \cdot h_{\text{CoG}} - \tag{4.38}$$

$$-l_{\text{R}} \cdot m_{\text{CoG}} \cdot g \cdot \cos\theta.$$

The F_{LF} and F_{LR} are traction forces, F_{ZF} and F_{ZR} are normal forces acting on the axles. The m_{CoG} is a vehicle mass, θ is slope angle. The center of gravity (CoG) position is defined by l_{F} , l_{R} and h_{CoG} dimensions. The F_{AR} is a air resistance and v_{CoG} is a vehicle speed.

The air resistance can be derived as:

$$F_{\text{AR}} = \frac{1}{2} \cdot \rho_{\text{A}} \cdot C_{\text{X}} \cdot S_{\text{X}} \cdot v_{\text{CoG}}^2, \tag{4.39}$$

where ρ_{A} is air density, C_{X} is air resistance coefficient and S_{X} is vehicle cross sectional area.

The Equations (4.36), (4.37) and (4.38) can be rewritten what gives normal forces determination [15]:

$$F_{\text{ZF}} = \frac{h_{\text{CoG}} \cdot (F_{\text{AR}} - m_{\text{CoG}} \cdot \sin\theta - m_{\text{CoG}} \cdot \dot{v}_{\text{CoG}}) + l_{\text{R}} \cdot m_{\text{CoG}} \cdot \cos\theta}{l_{\text{F}} + l_{\text{R}}}, \tag{4.40}$$

$$F_{\text{ZR}} = \frac{-h_{\text{CoG}} \cdot (F_{\text{AR}} - m_{\text{CoG}} \cdot \sin\theta - m_{\text{CoG}} \cdot \dot{v}_{\text{CoG}}) + l_{\text{F}} \cdot m_{\text{CoG}} \cdot \cos\theta}{l_{\text{F}} + l_{\text{R}}}. \tag{4.41}$$

---

[5]Green color match with Simulink inputs and magenta color match with Simulink outputs.
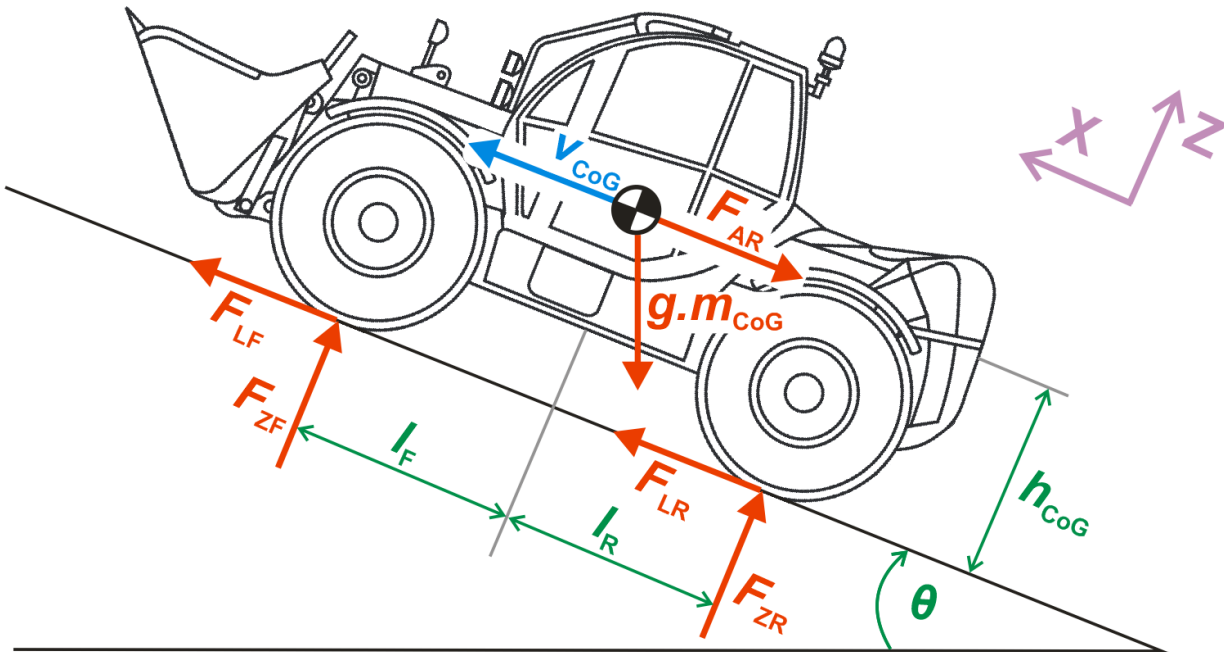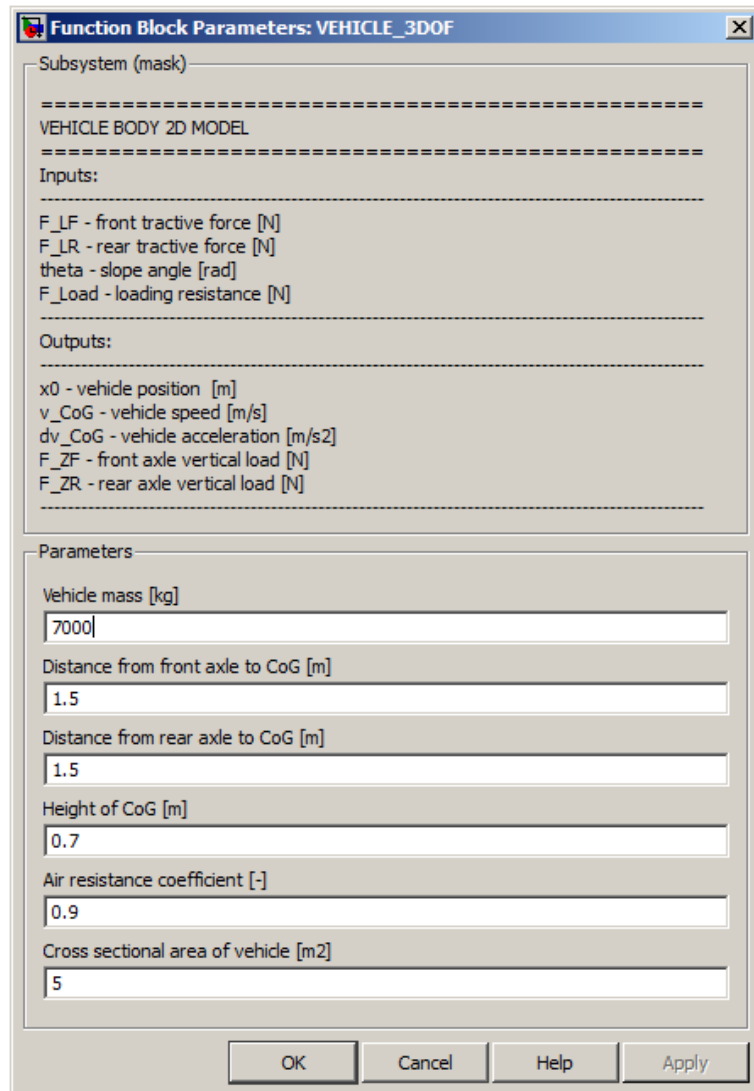
Figure 4.12: Forces acting on vehicle's body

The previous equations were implemented in MATLAB-Simulink (shown in Figure A.6). The inputs and outputs in Simulink (shown in Table 4.8) must be compatible with other Simulink blocks (subsystems). The initial conditions are set to: $v_{\text{CoG}} = 0.001$ m/s or $\omega_{\text{FL}} = 0.001$ rad/s. This simplification increases simulation speed. The vehicle body block allows simple setting of tunable parameters in subsystem mask shown in Figure 4.13. User can simply set up: vehicle mass, center of gravity position and vehicle cross sectional area.

VEHICLE BODY			
Signal	Description	Symbol	Unit
INPUTS	Longitudinal force from front axle	F_{LF}	N
	Longitudinal force from rear axle	F_{LR}	N
	Slope	θ	rad
OUTPUTS	Front axle normal load	F_{ZF}	N
	Rear axle normal load	F_{ZR}	N
	Vehicle (CoG) trajectory	x_0	m
	Vehicle (CoG) speed	v_{CoG}	m·s^{-1}
	Vehicle (CoG) acceleration	$\dot{v}_{\text{CoG}}$	m·s^{-2}

Table 4.8: Vehicle body inputs and outputs - forward drive[6]

---

[6]Green color match with Simulink inputs and magenta color match with Simulink outputs.

Figure 4.13: Vehicle body subsystem mask

5 Control algorithm of mobile working machine

In the previous Chapter 4 mathematical and physical vehicle model was developed. This model is necessary for design, testing and optimalization of HST control. The control options of speed gears shift and diesel engine speed are assumed during HST control design. The HST control design includes following steps:

1. Definition of machine working cycle.
2. Definition of powertrain control modes.
3. Selection of HST control.

    (a) Selection of pump control.
    (b) Selection of motor control.

4. Design of control algorithms for HST (pump, motor).
5. Optimalization of algorithms.
6. Connection of algorithms.
7. Testing of final algorithm.
8. Verification of simulations results.

5.1 Description of MWM working cycle

The working cycle of MWM must be defined at the beginning of HST control design. The working cycle of MWM can be divided to two modes:

- First mode is vehicle transportation to workstation.
- Second mode is working on workstation.

Because each type of MWM has characteristic working cycle, a universal working cycle definition is impossible. For selected telehandler following modes are assumed: mode A represents vehicle transportation to workstation (uphill and downhill driving) and mode B represents working on workstation (stuff loading and unloading) as it is shown in Figure 5.1.
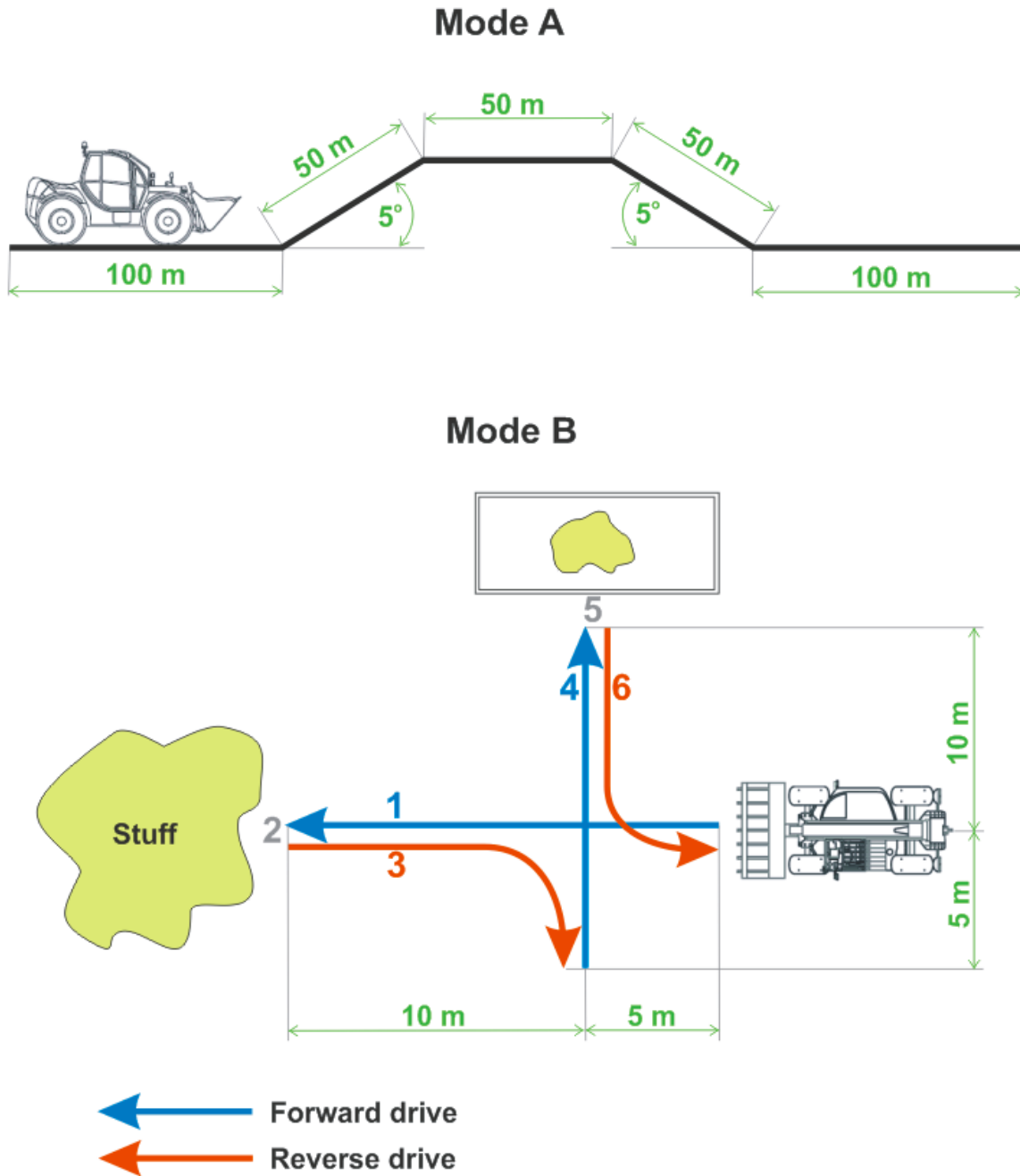
Figure 5.1: Working cycle - Mode A and Mode B, (1,4 - forward drive, 3,6 - reverse drive, 2 - loading, 5- unloading)

5.2 Description of driving modes

Control modes of MWM are methods how to control the powertrain modes of MWM. In vehicles equipped with HST it is possible to change driving mode according to driver or safety demands. It is means that the driver can change MWM driving mode by pressing correspondent button in dependence on current situation.

A regulation of pump and motor is typical for telescopic loaders (telehandlers), when the pump and motor displacement is dependent on the diesel engine speed. The primary regulation (regulation of pump) is active by lower engine speed. The secondary regulation (regulation of motor) is active by the higher engine speed. The primary and secondary regulation is not active together. During engine speed increasing the pump displacement is increasing too (primary regulation). When all the options of primary regulation are ran out, the secondary regulation starts to be involved, that it is mean that the displacement of motor is reduced. By decreasing of the engine speed the HST control acts analogue.

Sophisticated control algorithms were developed by tractor producer Fendt (Vario transmission) and John Deere (AutoPowr transmission) [2].

- Normal drive mode
- Optimal drive mode

Normal drive mode is shown in Figure 5.2. The speed is controlled by accelerator pedal; the speed gear shift is controlled by joystick by this mode. The swashplate and bent axis angles are linear dependent on the engine speed (as shown in Figure 5.3). The beginning of secondary regulation (n_{ps}) is in 1600 min^{-1}, where the maximal engine torque is available. This setting of HST control allows secure machine operation. There is no focus on operation costs. The working mode can be used in the working cycle or machine transportation to workstation.

Optimal drive mode is shown in Figure 5.4. This driving mode allows vehicle control only with joystick. The pump, motor, engine and gearbox are controlled in dependence on driver demand. The swashplate and bent axis angles are linear dependent on the engine speed (as shown in Figure 5.5). The beginning of secondary regulation is in 1100 min^{-1}. This value was adjusted by simulations. This setting of HST control allows decrease of fuel consumption. It is optimal mode regarding operation costs. The working mode can be used in the working cycle (the automatic gear shift is blocked) or machine transportation to workstation.
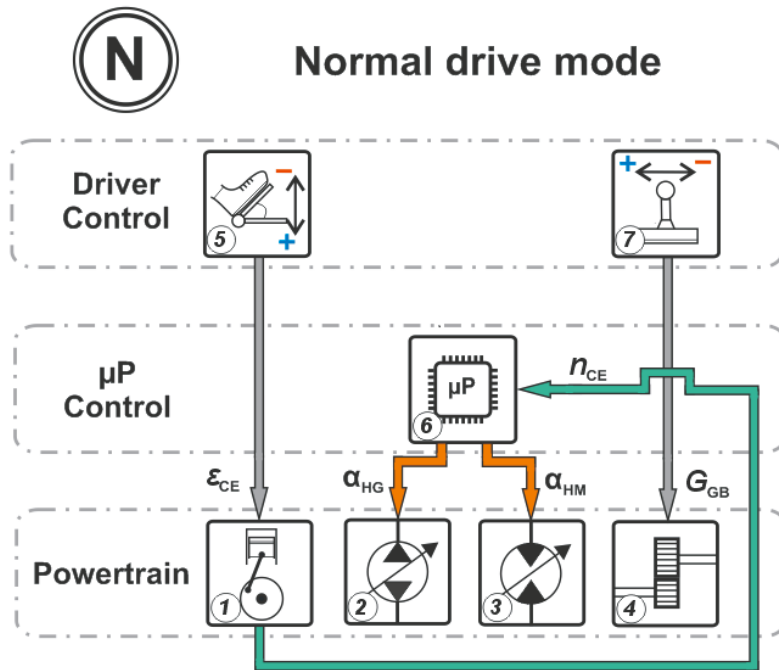
Figure 5.2: Normal drive mode: 1-Diesel engine, 2-Pump, 3-Motor, 4-Gearbox, 5-Accelerator pedal control, 6-Microprocessor, 7-Joystick control
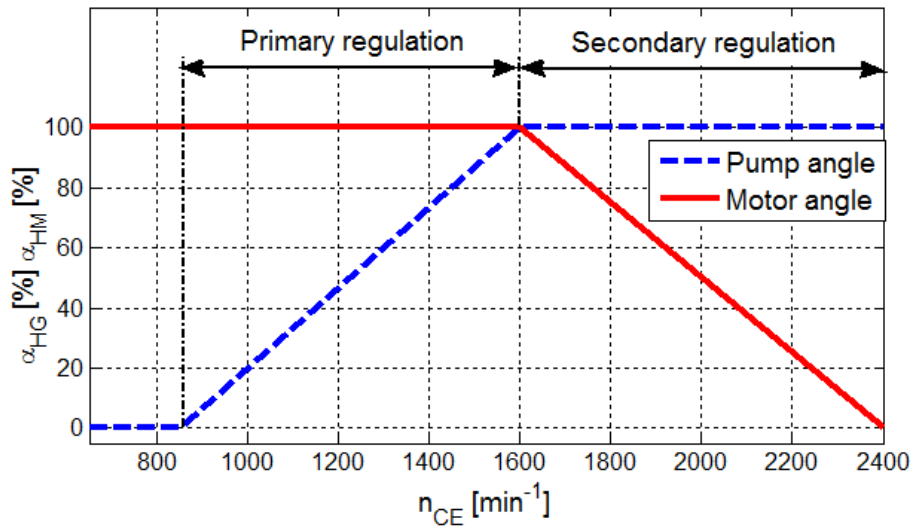

Figure 5.3: Normal drive mode : Pump α_{HG} angle and Motor α_{HM} angle vs CE speed
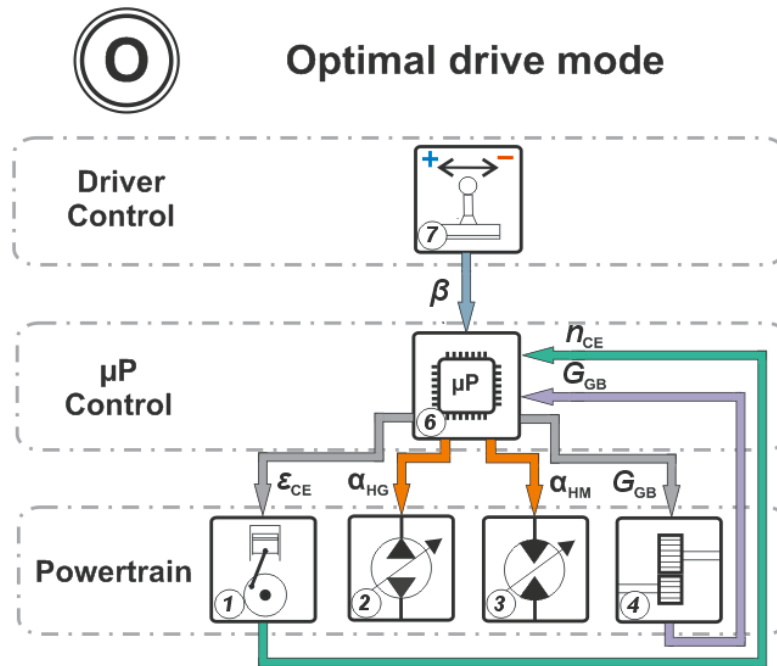
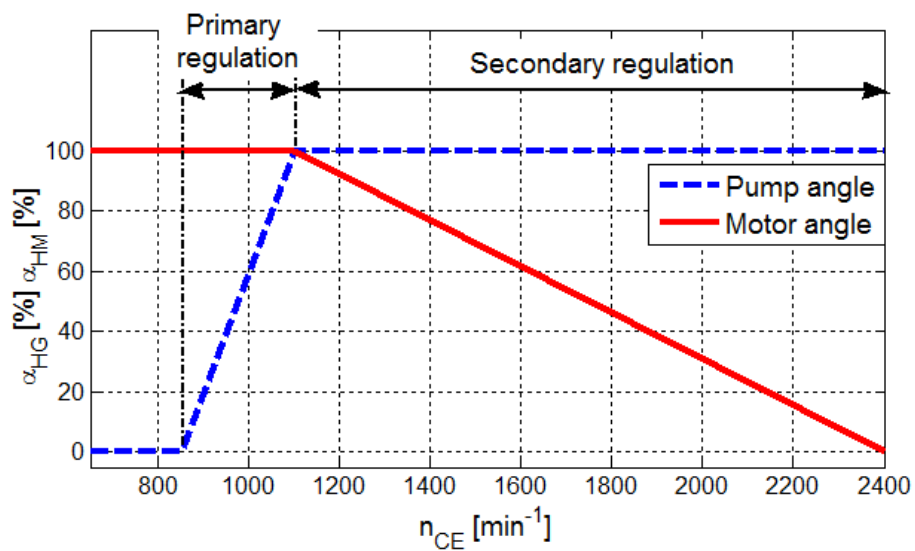Figure 5.4: Optimal drive mode: 1-Diesel engine, 2-Pump, 3-Motor, 4-Gearbox, 6-Microprocessor, 7-Joystick control

Figure 5.5: Optimal drive mode : Pump α_{HG} angle and Motor α_{HM} angle vs CE speed

5.3   Control of hydrostatic transmissions

The controlled pumps and motors must contain hydraulic, electric or electro-hydraulic control system. This control system drives swashplate angle, bent axis angle, valves etc. in dependence on the input signals (current, pressure, voltage ...). Basic control options of pump and motor are following:

- Two-position control.

- Multi-position control.

- Proportional control (continuous control).

The Sauer-Danfoss offers about 5 types of control for selected H1 (frame 78 cm^3) pump. For example: *Electrical Displacement Control* (EDC) ,*Forward-Neutral-Reverse electric control* (FNR) and *Non Feedback Proportional Electric Control* (NFPE). Designated control types are manufactured for 12 V and 24 V vehicle variants [9].

The selected Sauer-Danfoss motor S51 (frame 110 cm^3) can be combined with 14 control types approximately. For example: *Electro-hydraulic Two-Position Control* (E1B), *Hydraulic Two-Position Control* (TH), *Electro-hydraulic Proportional Control* (D8M1). Designated control types are manufactured for 12 V and 24 V vehicle variants [22].

5.4   Selection of pump control

The most suitable control type for our purposes is electric proportional control. This control type allows continuous change of pump displacement. Based on previous demands the *Electrical Displacement Control* (EDC) - A3 control was chosen for 24 V variant of vehicle (parameters are shown in Table 5.1).

Electrical Displacement Control Principle: *The Electrical Displacement Control (EDC)* consists of a pair of proportional solenoids on each side of a three position, four-way porting spool. The proportional solenoid applies a force input to the spool, which ports hydraulic pressure to either side of a double acting servo piston. Differential pressure across the servo piston rotates the swashplate, changing the pump's displacement from full displacement in one direction to full displacement in the opposite direction. EDC Operation

HI EDC is current driven control (as shown in Figure 5.6) requiring a Pulse Width Modulated (PWM) signal. Pulse width modulation allows more precise control of current to the solenoids. The PWM signal causes the solenoid pin to push against the porting spool, which pressurizes one side of the servo piston, while draining the other. Pressure differential across the servo piston moves the swashplate. A swashplate feedback link, opposing control links, and a linear spring provide swashplate position force feedback to the solenoid. The control system reaches equilibrium when the position of the swashplate exactly balances the input command from the operator (solenoid). As hydraulic pressures in the operating loop changes with load, the control assembly and servo/swashplate system work constantly to maintain the commanded position of the swashplate.

When the control input signal is either lost or removed, or if there is a loss of charge

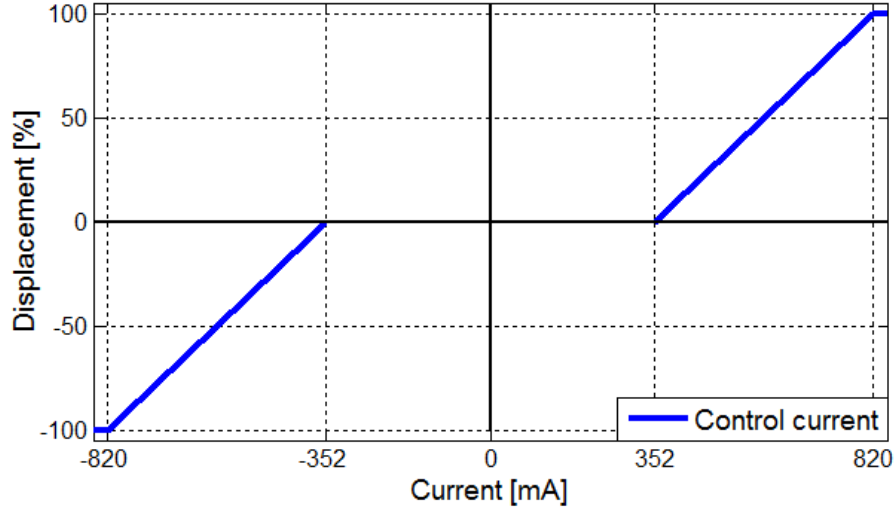pressure, the spring-loaded servo piston will automatically return the pump to the neutral position [9].

Figure 5.6: Pump displacement vs. control current [9]

Parameter	Value	Unit	Parameter	Value	Unit
Voltage	24	V	Coil resistance at 20°C	14.20	Ω
Threshold current (+/-)	350	mA	Coil resistance at 80°C	17.52	Ω
End current (+/-)	820	mA	PWM frequency range	70 to 200	Hz
Maximum current	920	mA	Recommended PWM freq.	100	Hz
Rated power	18	W	Inductance	140	mH

Table 5.1: H1 A3 EDC Electrical Specifications [9]

5.5   Selection of motor control

The most suitable control type for our purposes is electric proportional (electro-hydraulic) control. This control type allows continuous change of motor displacement as well as pump control. According to Sauer-Danfoss catalogue [22] for telehandler application *Electro-hydraulic Proportional Control* is used. Since 24 V vehicle variant is expected, D8 type (parameters are shown in Table 5.2) is chosen.

Electro-hydraulic Proportional Control principle: Displacement can be changed electrohydraulically (as shown in Figure 5.7) under load in response to an electrical signal from minimum displacement to maximum displacement and vice versa. The displacement

changes are proportional to the electrical signal. The electrical signal must be a pulse-width modulated (PWM) signal [22].

Electro-hydraulic Proportional Control is equipped with *Pressure Compensator Override* (PCOR). The control can be overridden by PCOR using high loop pressure. When the high pressure level equals to PCOR start pressure setting, the PCOR valve is activated. The motor displacement increases. This causes decreasing of system pressure to acceptable value and ensures optimal power utilization throughout the entire displacement range of the motor. PCOR start pressure is adjustable from 110 to 370 bar [22].

Electro-hydraulic Proportional Control should be equipped with *Hydraulic Brake Pressure Defeat* system or *Electric Brake Pressure Defeat* system. Brake Pressure defeat is not important for our simulations.
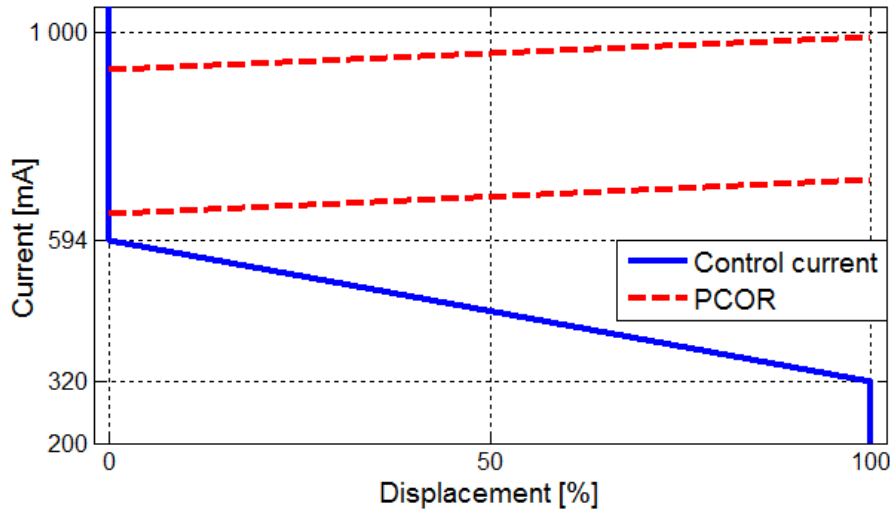

Figure 5.7: Motor displacement vs. control current [22]

Parameter	Value	Unit	Parameter	Value	Unit
Voltage	24	V	Coil resistance at 20°C	21.2	Ω
Start current (+/-)	320	mA	Coil resistance at 80°C	NA	Ω
End current (+/-)	594	mA	PWM frequency range	100 to 200	Hz
Maximum current	750	mA	Recommended PWM freq.	100	Hz
Rated power	NA	W	Inductance	NA	mH

Table 5.2: S51 D8 Electrical Specifications [22]

5.6 Control algorithm model

The developed HST control is based on the previously mentioned driving modes. In the normal driving mode vehicle speed is controlled by accelerator pedal. The demanded engine speed is output from control block (subsystem) to diesel engine. The engine speed feedback is used for displacement control of pump and motor (as shown in Figure 5.2). A shift of speed gear upwards is realized with forward joystick movement and a shift of speed gear downwards is realized with reverse joystick movement.

The optimal drive mode operates like a normal mode but with two differences. First difference is in the way how the vehicle speed (CE speed) is set. The speed in the optimal mode is controlled by joystick. The swashplate angle and bent axis angle dependence on the engine speed is shown in Figure 5.4. Second difference is automatic speed gear shift in the optimal drive mode. The automatic speed gear shift is dependent on the engine speed analogous to pump and motor displacement. It can be switched off.

Both drive modes are prepared to reversal drive and braking with HST. During reversal drive the displacement of pump is opposite. The developed model of HST control is shown in Figure A.7. The inputs and outputs in Simulink (shown in Table 5.3) must be compatible with other Simulink blocks (subsystems).

The model block of HST allows simple setting of tunable parameters in subsystem mask. User can simply set up: HST linear regulation curve and specifications of gear shift control in the optimal drive mode.

HST CONTROL			
Signal	Description	Symbol	Unit
INPUTS	Control drive mode	$Control$	-
	Work mode (for Optimal drive mode)	$Work\ ON/OFF$	-
	Engine speed	n_{CE}	min^{-1}
	Joystick position	β	%
	Accelerator pedal position	ε_{CE}	%
	Reverse drive	reverse	-
	Brake pedal position	γ	%
OUTPUTS	HG angle	α_{HG}	%
	HM angle	α_{HM}	%
	Actual gear	G_{GB}	-
	Accelerator pedal position	ε_{CE}	%
	Front axle brake torque	T_{BF}	N·m
	Rear axle brake torque	T_{BR}	N·m

Table 5.3: Diesel engine inputs and outputs[1]

---

[1]Green color match with Simulink inputs and magenta color match with Simulink outputs.

6   Mobile working machine model simulation

6.1   Model testing of mobile working machine

Model simulation consists of several types of simulation. Because of large number of simulations only some simulations (tests) and working cycles (Mode A, Mode B) were selected. The used simulation parameters are shown in Table A.1. The model (for simulations/tests) is combined from blocks created in Simulink. The model consists of: diesel engine block, HST block, gearbox block, central differential gear block, wheel blocks and control block as shown in Figure A.8.

Kick-down simulation (shown in Figure 6.1) - is basic test of kick-down (driver pushes the accelerator pedal to the floor) response. During simulation the first speed gear is engaged. At the beginning of the simulation the accelerator pedal is t pushed to the floor (kick-down) rapidly. The vehicle uses almost all engine power. A reaching of the maximal engine power and speed is impossible because of proportional control which is used for speed regulation.

Simulation of vehicle's acceleration and deceleration (shown in Figure 6.2) - is simulation which tests response of system to sequential accelerating and decelerating commands. During simulation the first speed gear is engaged, the vehicle is not loaded, and it drives on field path. The normal drive mode is selected. The vehicle speed copies diesel engine speed like in the previous kick-down test.

Maximal speed simulation (shown in Figure 6.2) simulates vehicle maximal speed response. During simulation the vehicle is not loaded and it drives on field path. The normal drive mode is selected. At the beginning of the simulation the accelerator pedal is rapidly pushed to the floor. After reaching of maximal speed by first gear, the gear shifts to higher gear. During the speed gear shift the engine speed shallow oscillates a little bit. It is caused by step gear ratio change.

The basic vehicle testing showed that model's behavior is realistic also by intuitive presumptions and MWM producer's data. Specific limitations of speed gear shift and vehicle start must be taken into account during simulation results evaluation. Front and rear wheels slip oscillating and following torque oscillations are typical for vehicle start as shown in Figure 6.2. These undesirable oscillations are caused by structure of equations used in the powertrain model.
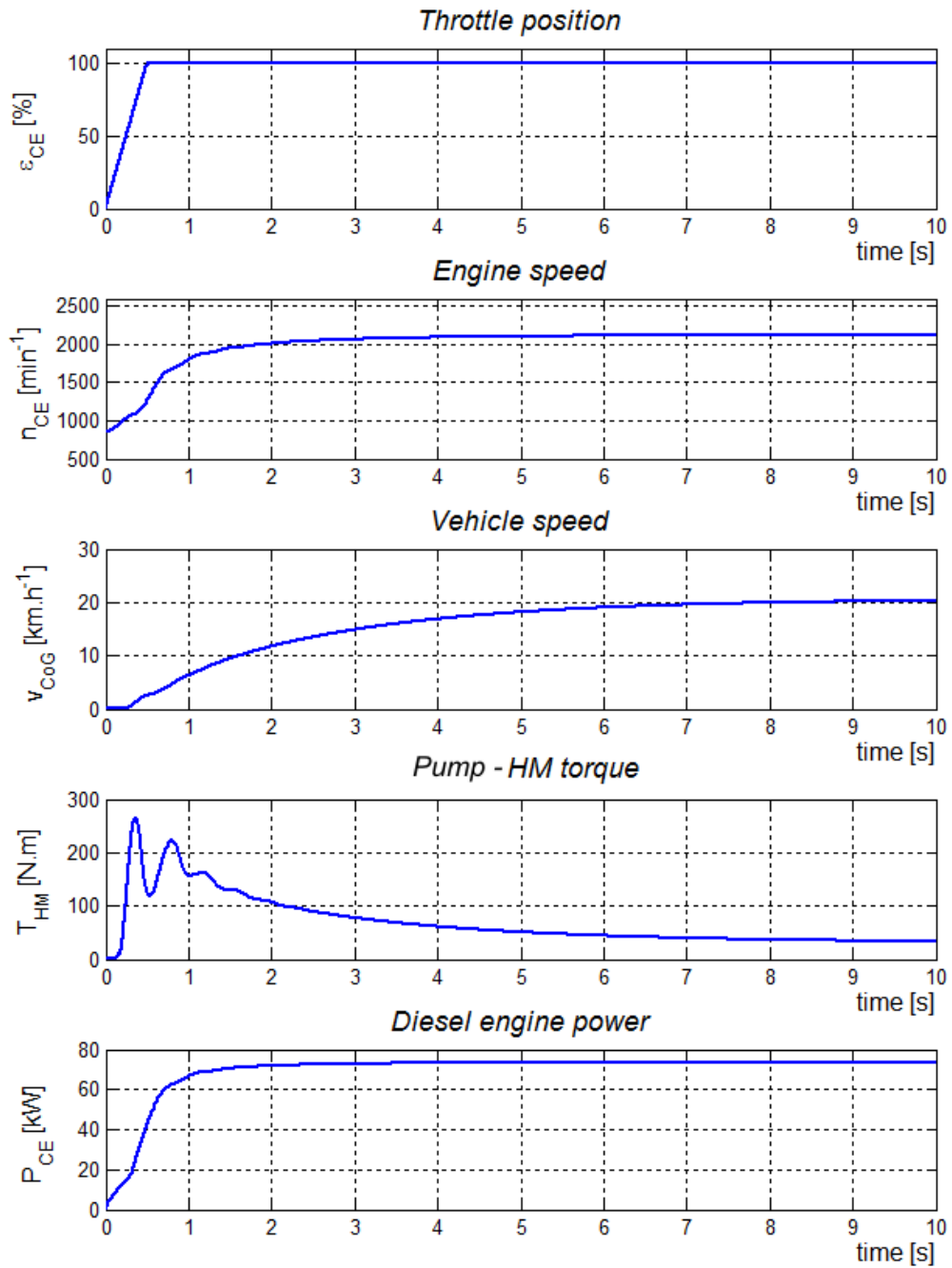
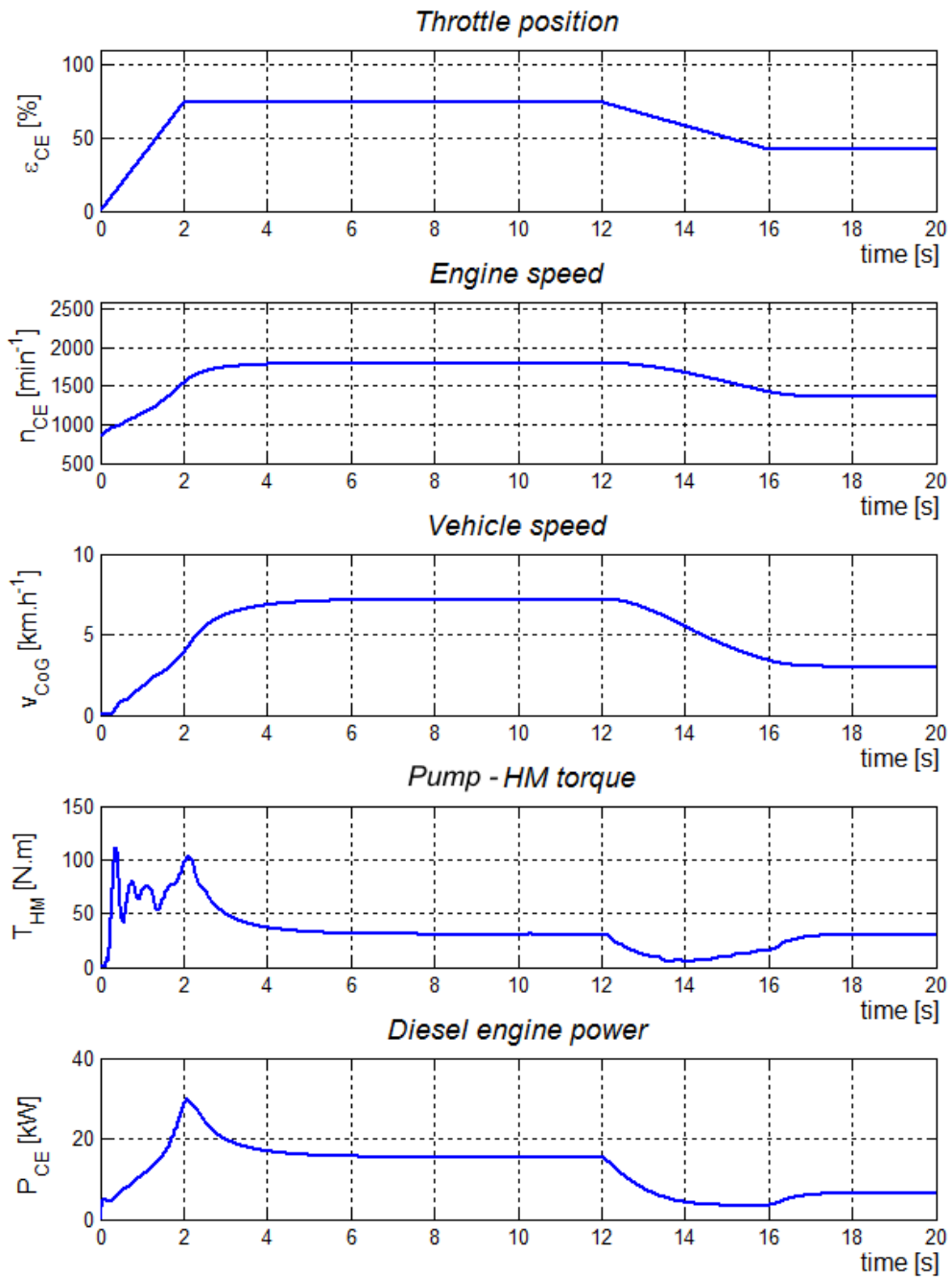Figure 6.1: Kick-down simulation - gear number 1 and normal drive mode

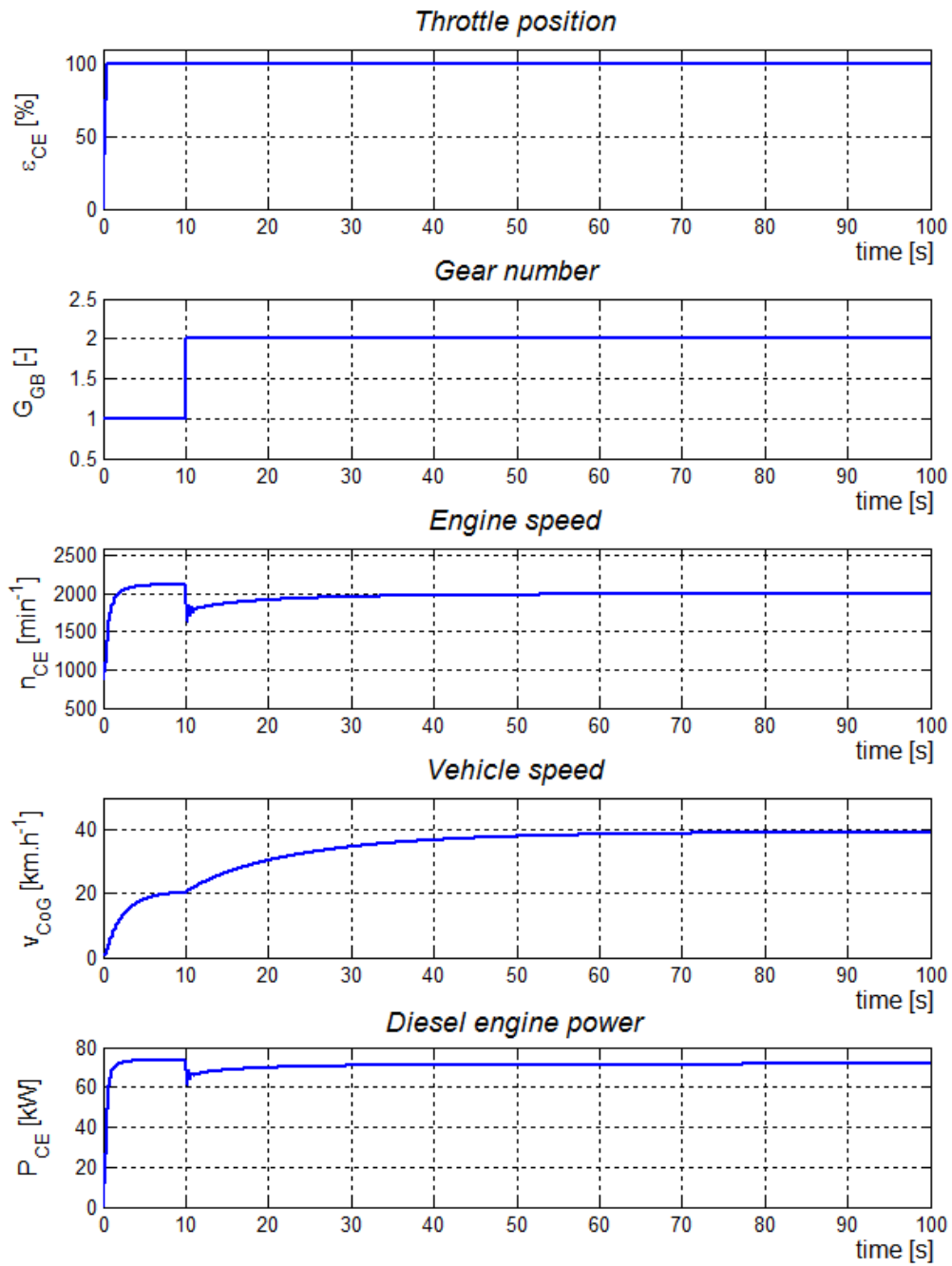Figure 6.2: Accelerating and decelerating simulation - gear number 1 and normal drive mode

Figure 6.3: Maximal speed simulation - field path

6.2 Comparison between simulated results and results of other authors

The model verification can be considered adequate only in comparison with measured data. The measure data is not available now. For this reason it is necessary to confront simulated results with results of other authors. However there are only few simulation results for comparison. For this purpose simulation results from Tinker [24] are taken. Tinker simulated powertrain of Caterpillar wheel loader. His simulation results are compared with measured data as shown in Figure 6.4. As it is shown in this figure forward and reverse drives are simulated. The first graph represents position of accelerator pedal [%], the second graph represents current gear number [-], the third graph represents engine speed [min^{-1}], the next graph represents wheel speed [min^{-1}] and the last graph represents torque from wheels [Nm].

The simulation of selected machine is shown in Figure 6.5. The last two graphs are speed and torque of front wheels/axle.

With respect to different MWM design and selected telehandler it is impossible to compare absolute values. Another problem is an unavailability of some parameters and significant differences (for example vehicle weight) between compared vehicles. Therefore only shapes of characteristics can be compared. The tendencies of simulated characteristics are almost identical as shown in Figure 6.5 and 6.4. Based on this comparison, it can be assumed that simulated results are realistic, off course with respect to previously mentioned problematic areas of control and vehicle's acceleration.
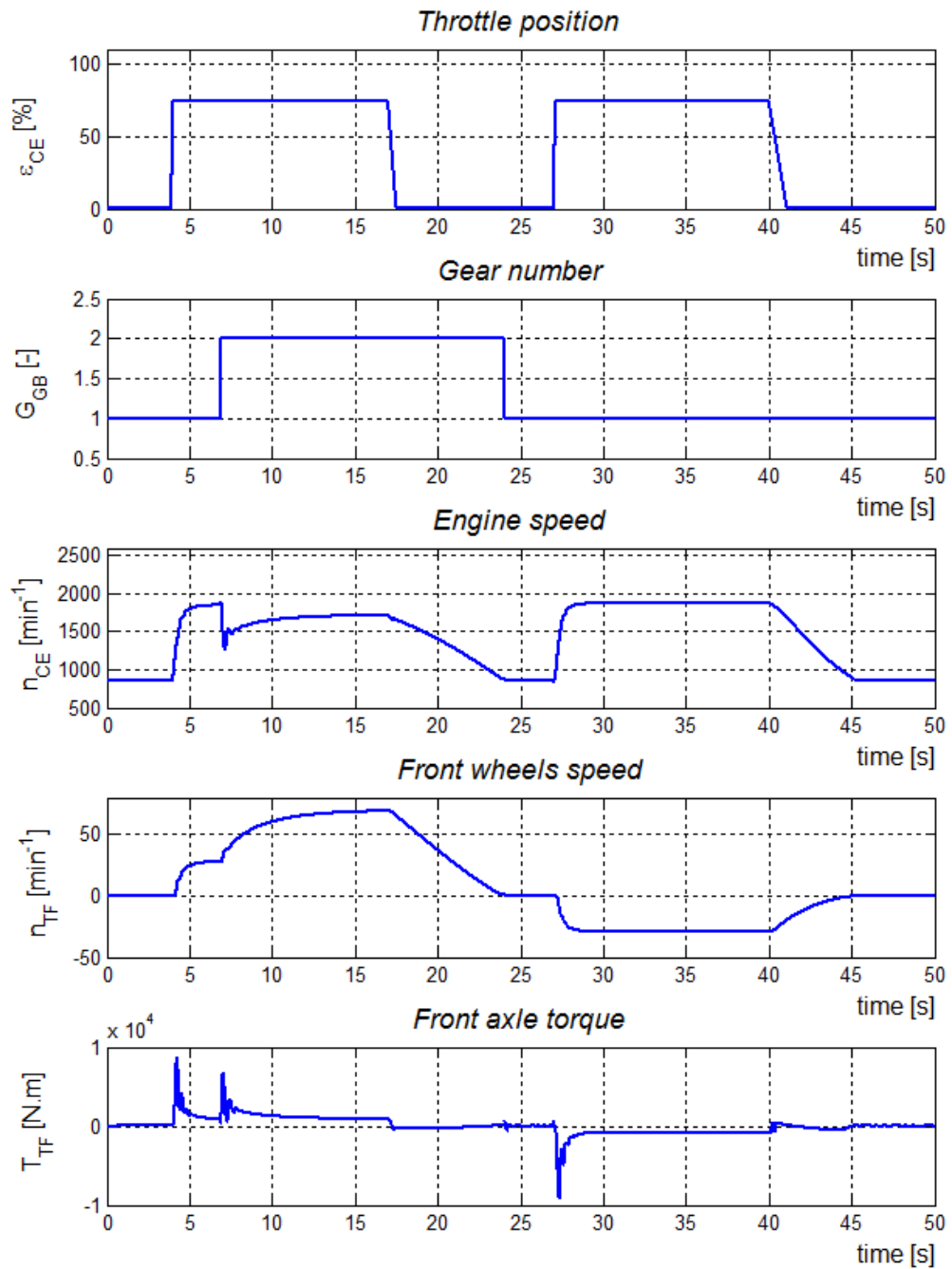
Figure 6.4: Caterpillar wheel loader - simulation and test results [24]
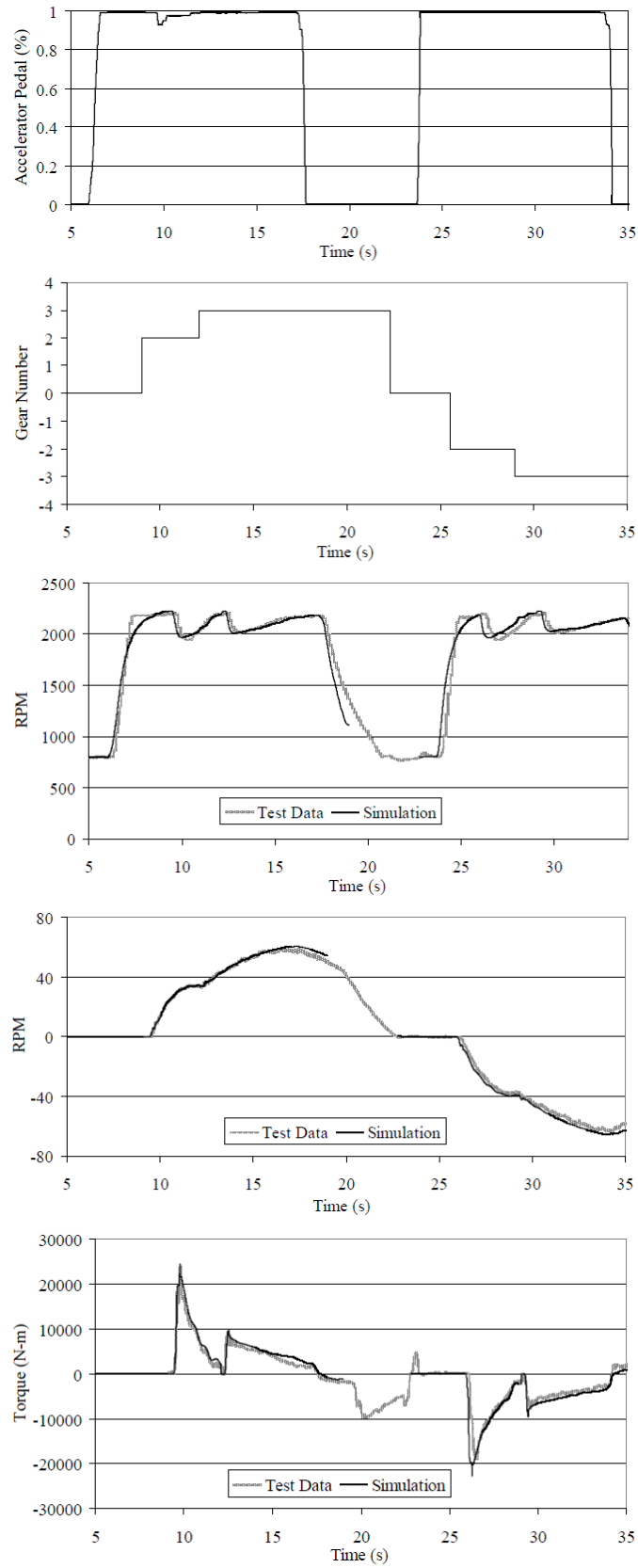
Figure 6.5: Telehandler simulation for comparison with Tinker's results

6.3   Working cycle simulation - Mode A

A testing of vehicle's simulation model according to mode A is shown in Figure 5.1. The vehicle was tested for various driver demands and various speeds. The road surface was assumed to be a dry field road. The MWM was unloaded. During the testing of simulation model by normal drive mode a change of speed gear in 4th second was simulated. The optimal drive mode shifted speed gears automatically in dependence on diesel engine speed. The demanded engine speed was set up by accelator pedal (in optimal drive mode by joystick) to demand values according to Table 6.1. Figure 6.6 represents simulation by selected vehicle

NORMAL DRIVE MODE		
Demanded CE speed [min^{-1}]	Fuel consumption [l]	Range time [s]
1500	0.1610	280.5
1800	0.1322	150.3
2000	0.1216	98.4
2200	0.1246	61.6
OPTIMAL DRIVE MODE		
Demanded CE speed [min^{-1}]	Fuel consumption [l]	Range time [s]
1500	0.1874	398.0
1800	0.1141	110.6
2000	0.1150	77.1
2200	0.1083	51.5
OPTIMAL vs NORMAL DRIVE MODE		
Demanded CE speed [min^{-1}]	Fuel consumption [%]	Range time [%]
1500	+16.4	+41.9
1800	-13.7	-26.4
2000	-5.4	-21.6
2200	-13.1	-16.4

Table 6.1: Normal and optimal control algorithm comparison for test range - Mode A

parameters during mode A. In this simulation the normal drive mode of powertrain control is active (vehicle/engine speed is set up by accelerator pedal). Figure 6.7 represents previous simulation with optimal drive mode of powertrain control (vehicle/engine speed is set up by joystick).

The Table 6.1 represents comparison between normal drive mode and optimal drive mode during mode A simulation. As it is shown in this figure the drive mode (setting of HST control) can significantly influence vehicle performance and operating costs. On the basis of intuitive premises and accessible information of telescopic loader's from manufacturers, obtained results can be considered as realistic. The simulation results must be considered

carefully at the beginning of simulation. According to Table 6.1 it can be deduced, that for higher engine speed (vehicle speed) the optimal drive is more suitable in working cycle - Mode A.
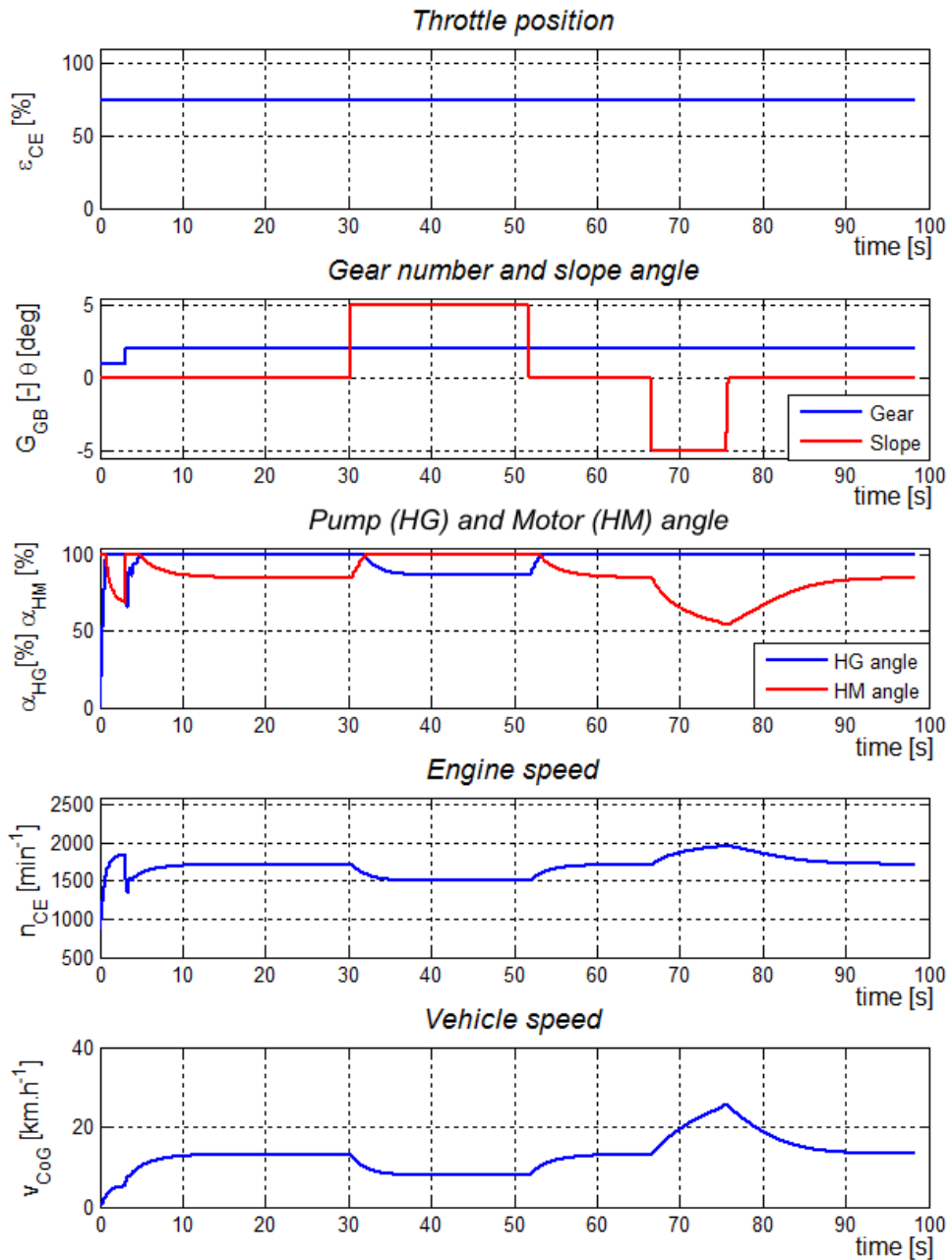

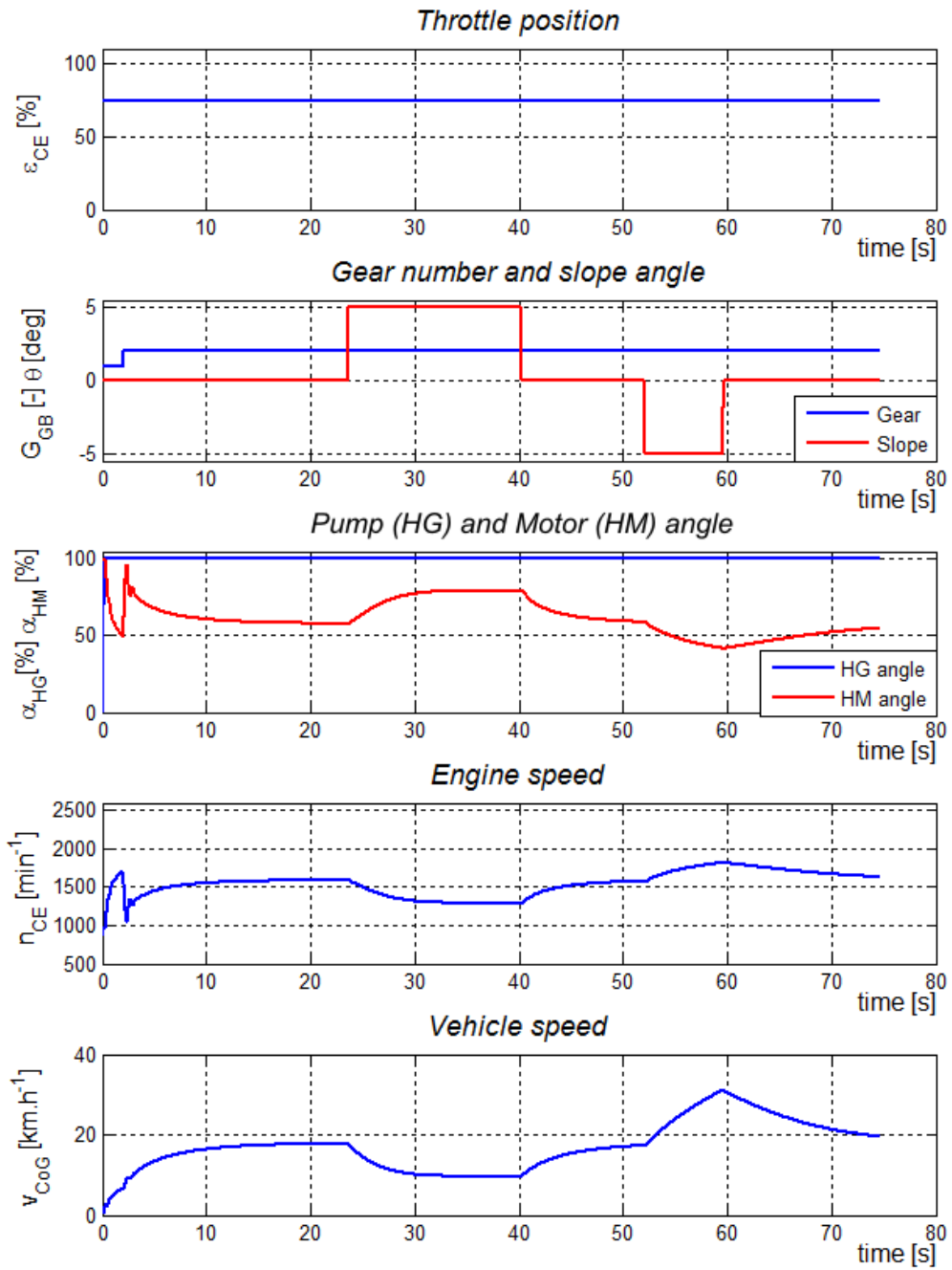Figure 6.6: Mode A simulation - Normal drive mode - field path

61

Figure 6.7: Mode A simulation - Optimal drive mode - field path

6.4   Working cycle simulation - Mode B

The testing of MWM powertrain model according to working cycle - mode B is shown in Figure 5.1. The road surface was assumed to be a field road. Influence of cornering drive was neglected. The work function (loading soil with dipper) was simulated as force load (2000 N) acting on the vehicle last two meters of forward vehicle drive by loading the soil. The vehicle load from soil's weight was simulated as a vehicle's mass increase (+500 kg) from the moment of loading till unloading as illustrated in Figure 5.1. During the simulation the first speed gear was engaged. The demanded engine speed was set up by accelerator pedal (in optimal drive mode by joystick). The maximal demanded value of the engine speed was 2000 min^{-1}. The characteristic of demanded engine speed was set up so that the vehicle could drive required distance without using mechanical brakes.

NORMAL DRIVE MODE			
Loading resistance [N]	**Load [kg]**	**Fuel consumption [l]**	**Range time [s]**
2000 (13m-15m)	500 (15m-45m)	0.0356	70
OPTIMAL DRIVE MODE			
Loading resistance [N]	**Load [kg]**	**Fuel consumption [l]**	**Range time [s]**
2000 (13m-15m)	500 (15m-45m)	0.0276	62
OPTIMAL vs NORMAL DRIVE MODE			
Loading resistance [N]	**Load [kg]**	**Fuel consumption [%]**	**Range time [%]**
2000 (13m-15m)	500 (15m-45m)	-22.5	-11.4

Table 6.2: Normal and optimal control algorithm comparison for tested range - Mode B

The results of simulation for mode B and normal drive mode (engine speed is set up by accelerator pedal) are shown in Figure 6.8. The Figure 6.9 represents results of the same test but for optimal drive mode (engine speed is set up by joystick).

Analogous to previous tests obtained results can be considered as realistic (with respect to used parameters and equations). The test results must be again considered carefully at the beginning of simulation. An influence of the loading and weight increase was minimal. The differences can be detected only by detailed search.

The Table 6.2 represents comparison between normal drive mode and optimal drive mode during mode (working cycle) B simulation. Drive mode (setting of HST control) again significantly influenced simulation results. The loading with enabled optimal drive mode significantly decreased fuel consumption and loading cycle time.

From this and previous tests we can assume that the reduction of fuel consumption can be done by suitable modification of pump and motor control characteristics. It can be deduced, that the HST setting in the optimal drive is more suitable. For selected application and testing cycles the using of primary regulation is more suitable for lower engine speed and smaller speed range.
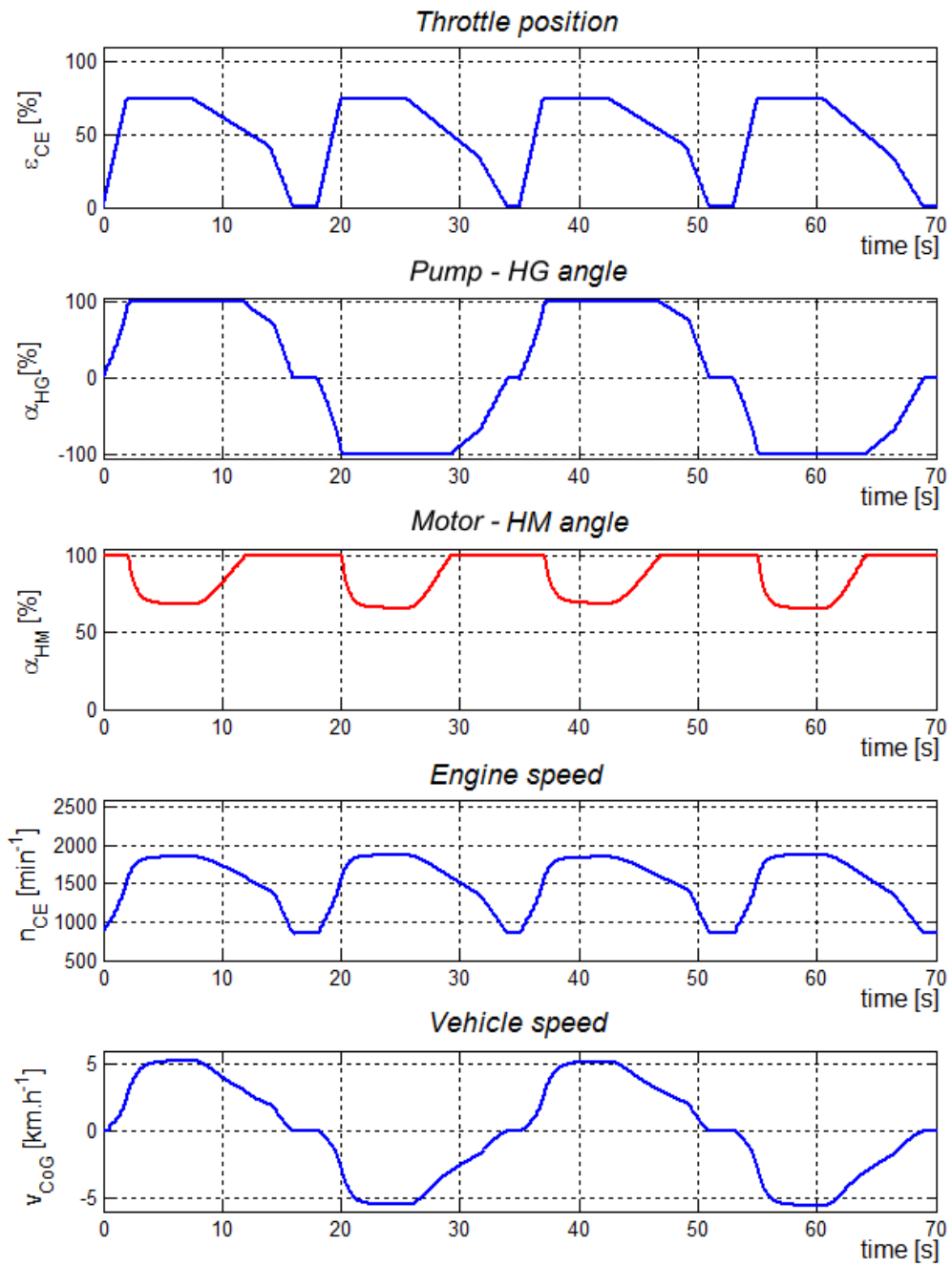
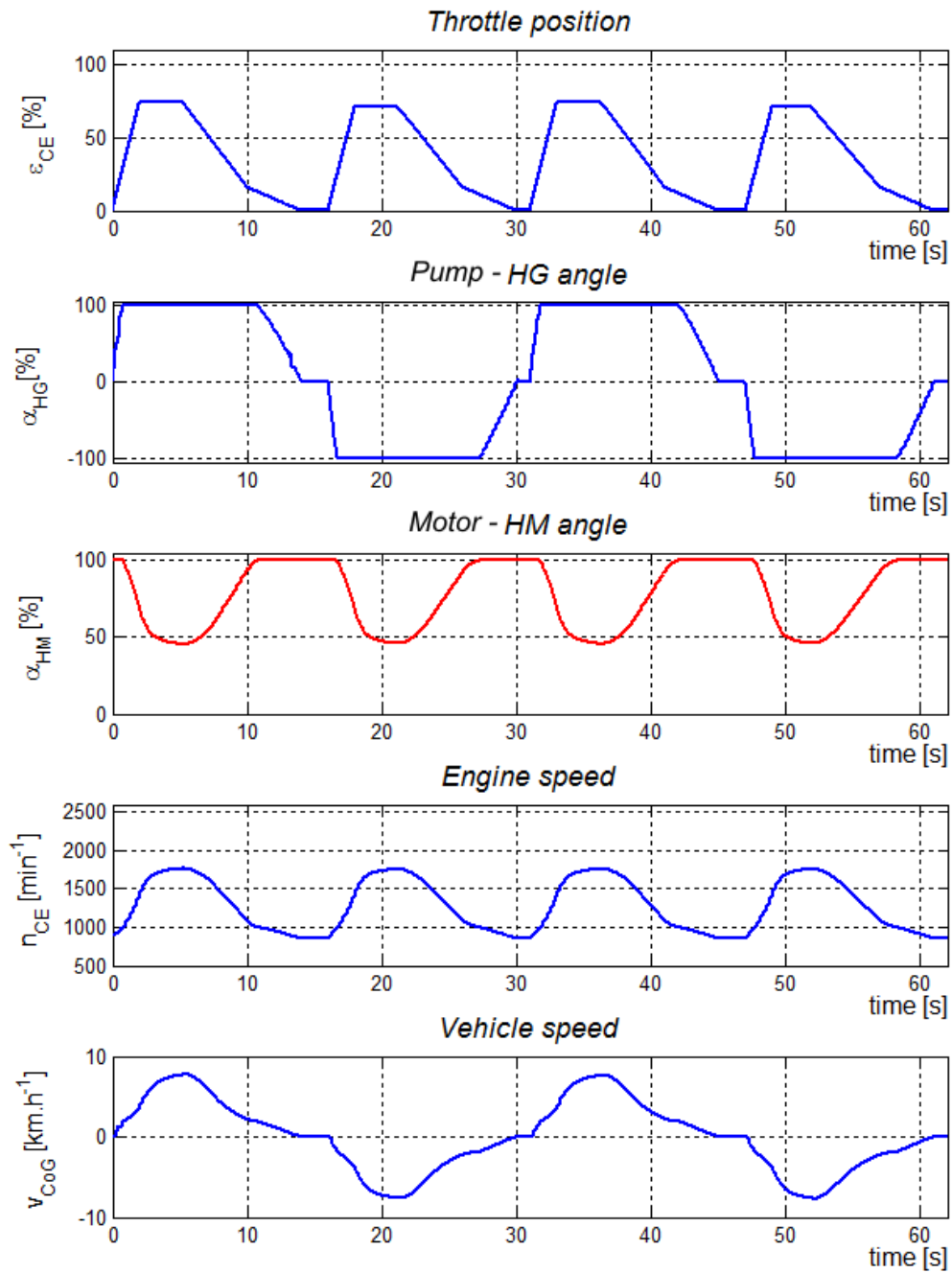Figure 6.8: Mode B simulation - Normal drive mode - field path

Figure 6.9: Mode B simulation - Optimal drive mode - field path

7 Conclusion and future work

In this thesis the mathematical and physical model of four wheel vehicle powertrain was created. Individual subsystems: diesel engine, hydrostatic transmission, gearbox, central differential gear, wheels, vehicle chassis and control were modeled separately by blocks. Modular structure increased speed and efficiency of MWM powertrain modeling. The individual blocks were created in MATLAB-Simulink program. A model of each subsystem (block) was equipped with mask, what increased user's comfort of parameters setting.

Detailed modeling of subsystem dynamics is difficult and imprecise because of model complexity and difficulties by acquiring of some parameters. For example the tire modeling is one of the most difficult fields of vehicle's modeling nowadays. Almost all modeled subsystems are non-linear.

The developed model shows strong non-linear behavior, which decelerates simulation mainly at the beginning.

The designed linear control algorithm shows relatively promising results. But it is still only base conception of the control algorithm. All performed simulations show acceptable results however in some cases (start, gear shift) it is necessary to consider physical and mathematical complexity of model's structure. During the simulation, it is important to know relationships and principles behind the user interface of these blocks, otherwise the simulation results can be misinterpreted by the engineer.

Developed models of subsystem contain some options, whose using is not confirmed yet (approximation of derivation, . . .). The tendency of this application settings results from need of including the inertia during acceleration

In the future, it is necessary to continue with developing of new blocks of drive and control and also with debugging of the initial conditions and parameter settings. Many of these were only guessed because of unavailability. This work provides good base for further model development of mobile working machine.

List of Symbols

Symbol	Description	Unit
C		
c_-	Burckhadt coefficients	-
C_{X}	air resistance coefficient	-
E		
e_{alw}	Allowed speed difference	min^{-1}
e_{w}	Rolling resistance radius	m
e_{CE}	Control deviation of engine speed	min^{-1}
F		
f_{r}	Rolling resistance coefficient	-
fr_{CE}	Relative fuel rack position	-
fr_{PD}	Actual fuel rack position	-
$F_{\max}$	Maximal tractive force	N
F_{w}	Total tractive force	N
F_{AR}	Air resistance force	N
F_{L}	Longitudinal tractive force	N
F_{LF}	Front longitudinal tractive force	N
F_{LR}	Rear longitudinal tractive force	N
F_{Z}	Wheel normal force	N
G		
g_{CE}	Fuel consumption	$\mathrm{g\cdot kW}^{-1}\cdot \mathrm{h}^{-1}$
G_{GB}	Actual speed gear	-
H		
h_{CoG}	Height of CoG	m
I		
i_1	First speed gear ratio	-
i_2	Second speed gear ratio	-

i_{GB}	Gearbox ratio	-
i_{T}	Torque distribution ratio of central differential gear	-

J

J_{CE}	Engine moment of inertia	kg·m^2
J_{w}	Wheel moment of inertia	kg·m^2

K

K_{CE}	Proportional gain of engine speed regulator	-

L

l_{F}	Distance between front axle and CoG	m
l_{R}	Distance between rear axle and CoG	m

M

m_{CoG}	Vehicle mass	kg

N

n_{idl}	Engine idling speed	min^{-1}
n_{max}	Engine maximal speed	min^{-1}
n_{ps}	Speed when secondary regulation start	min^{-1}
n_{CE}	Engine speed	min^{-1}
n_{CL}	Speed from gearbox	min^{-1}
n_{DE}	Demanded engine speed	min^{-1}
n_{HM}	Speed to pump (hydromotor)	min^{-1}
n_{TF}	Speed from front differential gear/axle	min^{-1}
n_{TR}	Speed from rear differential gear/axle	min^{-1}
n^{M}	Motor speed	min^{-1}
n^{P}	Pump speed	min^{-1}
$n^{\mathrm{M}}_{\mathrm{max}}$	Maximal motor speed	min^{-1}
$n^{\mathrm{P}}_{\mathrm{max}}$	Maximal pump speed	min^{-1}

P

p	Pressure	Pa
P_{max}	Maximal engine power	W
$P^{\mathrm{M}}_{\mathrm{C}}$	Motor corner power	W
$P^{\mathrm{M}}_{\mathrm{h}}$	Motor hydraulic power	W
$P^{\mathrm{M}}_{\mathrm{m}}$	Motor mechanical power	W
$P^{\mathrm{P}}_{\mathrm{h}}$	Pump hydraulic power	W
$P^{\mathrm{P}}_{\mathrm{m}}$	Pump mechanical power	W

Q

Q^{M}	Motor flow	$\mathrm{m^3 \cdot s^{-1}}$
Q^{P}	Pump flow	$\mathrm{m^3 \cdot s^{-1}}$

R

r_{w}	Wheel radius	m
R_{GM}	Gearing mechanism gear ratio	-
R_{HST}	Hydrostatic transmission gear ratio	-
R^{M}	Motor gear ratio	-
R^{P}	Pump gear ratio	-

S

s_{L}	Longitudinal slip	-
S_{X}	Vehicle cross sectional area	$\mathrm{m^2}$

T

t_{fr}	Fuel transport delay	s
T_{CL}	Torque from clutch	$\mathrm{N \cdot m}$
T_{CO}	Engine combustion torque	$\mathrm{N \cdot m}$
T_{B}	Wheel braking torque	$\mathrm{N \cdot m}$
T_{FE}	Engine friction torque	$\mathrm{N \cdot m}$
T_{GB}	Torque to central differential gear	$\mathrm{N \cdot m}$
T_{HM}	Torque from pump (hydromotor)	$\mathrm{N \cdot m}$
T_{ID}	Engine indicated torque	$\mathrm{N \cdot m}$
T_{T}	Wheel driving torque	$\mathrm{N \cdot m}$
T_{TF}	torque to front differential gear/axle	$\mathrm{N \cdot m}$
T_{TR}	Torque to rear differential gear/axle	$\mathrm{N \cdot m}$
T^{M}	Motor torque	$\mathrm{N \cdot m}$
T^{P}	Pump torque	$\mathrm{N \cdot m}$
$T^{\mathrm{M}}_{\max}$	Motor maximal torque	$\mathrm{N \cdot m}$
$T^{\mathrm{W}}_{\max}$	Wheel maximal torque	$\mathrm{N \cdot m}$

V

v_{CoG}	Vehicle (CoG) speed	$\mathrm{m \cdot s^{-1}}$
$v_{\max}$	Maximal vehicle (CoG) speed	$\mathrm{m \cdot s^{-1}}$
$v^1_{\max}$	Maximal vehicle first gear speed	$\mathrm{m \cdot s^{-1}}$
$v^2_{\max}$	Maximal second first gear speed	$\mathrm{m \cdot s^{-1}}$
$V^{\mathrm{M}}_{\max}$	Maximal motor displacement	$\mathrm{m^3}$
$V^{\mathrm{P}}_{\max}$	Maximal pump displacement	$\mathrm{m^3}$
$V^{\mathrm{P}}_{\min}$	Minimal pump displacement	$\mathrm{m^3}$

Z

Z	Number of speed gears	-

Greek

α_{HG}	Pump swashplate angle	%
α_{HM}	Motor bent axis angle	%
δ	Grade ability	%
ε_{CE}	Position of accelerator pedal	%
ζ^M	Motor regulation parameter	-
ζ^P	Pump regulation parameter	-
η_{GB}	Gearbox efficiency	-
η_{HST}	Hydrostatic transmission (HST) efficiency	-
η^M	Motor efficiency	-
η_{mh}^M	Motor mechanical-hydraulic efficiency	-
η_v^M	Motor volume efficiency	-
η^P	Pump efficiency	-
η_{mh}^P	Pump mechanical-hydraulic efficiency	-
η_v^P	Pump volume efficiency	-
θ	Slope angle	rad
μ_L	Longitudinal friction coefficient	-
ρ_A	Air density	kg· m^{-3}
τ	Swashplate or bent axis angle	°
τ_{max}	Maximal swashplate or bent axis angle	°
ω_{CE}	Engine speed	rad· s^{-1}
ω_w	Wheel speed	rad· s^{-1}

List of Abbreviations

CE	Combustion engine
CoG	Center of gravity
HST	Hydrostatic transmission
MWM	Mobile working machine
NA	Not available
PWM	Pulse width modulation
RQV	Speed regulator ("Regler Menge Vestell")

List of References

[1] BAKKER, E., NYBORG, L., PACEJKA, H. *Tyre Modelling for Use in Vehicle Dynamics Studies.* [s.l.]: [s.n.], c1987. 15 p. Society of Automotive Engineers, Inc.

[2] BAUER, F., SEDLÁK, P., ŠMERDA, T. *Traktory.* 1st edition. Praha: Profi Press, 2006. 192 p. Mendelova zemědělská a lesnická univerzita v Brně. ISBN 80-86726-15-0.

[3] BECKERS, J. *Matlab Simulink modelling of a hybrid vehicle.* [s.l.]: [s.n.], 2005. 21 p. Technische Universiteit Eindhoven. Ready from WWW:<http://alexandria.tue.nl/repository/books/613145.pdf>.

[4] BITEUS, J. *Mean Value Engine Model of a Heavy Duty Diesel Engine.* [s.l.]: [s.n.], 2004. 34 p. Department of Electrical Engineering Link¨opings universitet. Ready from WWW: <http://www.vehicular.isy.liu.se/Publications/Reports/04_R_2666_JB.pdf>. .

[5] CARLSSON, E. *Modeling Hydrostatic Transmission in Forest Vehicle.* [s.l.], 2006. 71 p. Thesis leader Anton Shiriaev. Ready from WWW: <http://www.diva-portal.org/diva/getDocument?urn_nbn_se_liu_diva-6864-1__fulltext.pdf>.

[6] CARTER, D. *Load modeling and emulation for an earthmoving vehicle powertrain.* [s.l.], 2003. 264 p. University of Illinois at Urbana-Champaign. Thesis leader Prof. Andrew Alleyne. Ready from WWW: <http://mr-roboto.me.uiuc.edu/ARGWeb/Publications/Theses/MS%20Theses/Carter_MS.pdf>.

[7] DONALD, M. *Design of a Vehicle Model and Traction Control System for a Drag.* [s.l.], 2007. 94 p. Rensselaer Polytechnic Institute. Project Adviser Ernesto Gutierrez-Miravete.

[8] GUZZELLA, L., AMSTUTZ, A. *The QSS Toolbox Manual.* [s.l.]: [s.n.], 2005. 63 p. IMRT Swiss Fedral Institute of Technology Zurich. Ready from WWW: <http://www.imrt.ethz.ch/research/qss>.

[9] *H1 Axial Piston Pumps 045/053 Single, 045/053 Tandem, 078 Single, 115/130 Single, 147/165 Single* [s.l.]: Sauer Danfoss, c2009. 204 p. Catalogue. Ready from WWW: <http://www.sauer-danfoss.com/stellent/groups/publications/documents/product_literature/11009999.pdf>.

[10] IVANTYSYN, J., IVANTYSYNOVA, M. *Hydrostatische Pumpen und Motoren.* Vogel Buchverlag, Würzburg, 1993

[11] KIENCKE, U., NIELSEN, L. *Automotive Control Systems: For Engine, Driveline, and Vehicle.* 2nd edition. [s.l.]: Springer-Verlag, c2005. 512 p. ISBN 3-540-23139-0.

[12] KOPÁČEK, J. *Mechanické a hydraulické převody. Hydraulické převody.* VŠB-Technická univerzita, Ostrava, 1996.

[13] KOREIS, J. *Řízení zatížení hnacího motoru regulačním převodem.* In. Převodová ústrojí a mechanismy DRIVE 97, Ostrava, 1997.

[14] KUČÍK, P., STRÁŽOVEC, I., KRIŠŠÁK, P. *Hydraulický prenos energie : Mobilné pracovné stroje.* 1st edition. Žilina: EDIS, 2000. 384 p. ISBN 80-7100-725-0.

[15] *Matlab Simulink: SimDriveline 1.* [s.l.]: The MathWorks, Inc., c2008. 118 p. User's guide. Ready from WWW: <http://www.mathworks.com/access/helpdesk/help/pdf_doc/physmod/drive/drive.pdf>.

[16] MUSSAEUS, M. *Control issues of hybrid and conventional drive lines.* [s.l.]: [s.n.], 1997. 38 p. Eindhoven University of Technology. Ready from WWW: <http://alexandria.tue.nl/repository/books/632048.pdf>.

[17] PRASETIAWAN, E. *Modeling, simulation and control of an earthmoving vehicle powertrain simulator.* [s.l.], 2001. 143 p. University of Illinois at Urbana-Champaign. Thesis leader Prof. Andrew Alleyne. Ready from WWW: <http://mr-roboto.me.uiuc.edu/Evps/theses/eko_thesis.pdf>.

[18] RILL, Gg. *Vehicle dynamics : Lecture notes.* [s.l.]: [s.n.], 2007. 167 p. Fachhochschule Regensburg, University of applied sciences, Ready from WWW:<http://homepages.fh-regensburg.de/~rig39165/skripte/Vehicle_Dynamics.pdf>.

[19] RILL, G. *Vehicle modeling by subsystems.* J. Braz. Soc. Mech. Sci. & Eng. [online]. 2006, vol. 28, no. 42008-10-27], pp. 430-442. Ready from WWW: <http://www.scielo.br/scielo.php?script=sci_arttext&pid=S1678-58782006000400007&lng=&nrm=iso>. ISSN 1678-5878. doi: 10.1590/S1678-58782006000400007.

[20] SEMETKO, J. *Mobilné energetické prostriedky 2: Mechanizmy vozidiel.* Bratislava: Príroda, 1985. 363 p.

[21] SEMETKO, J. *Mobilné energetické prostriedky 3: Traktory a automobily* Bratislava: Príroda, 1986. 453 p.

[22] *Series 51, Series 51-1, Bent Axis Variable Displacement Motors, Technical Information* [s.l.]: Sauer Danfoss, c2003. 112 p. Catalogue. Ready from WWW: <http://www.sauer-danfoss.com/stellent/groups/publications/documents/product_literature/520l0440.pdf>.

[23] STRANDH, P. *Combustion Engine Models for Hybrid Vehicle System Development.* [s.l.], 2002. 80 p. Division of Combustion Engines, Department of Heat and Power Engineering, Lund Institute of Technology. Thesis leader Rolf Egnell. Ready from WWW: <`http://www.iea.lth.se/publications/Theses/petter.pdf`>.

[24] TINKER, M. *Wheel loader powertrain modeling for real-time vehicle.* [s.l.], 2006. 116 p. University of Iowa. Thesis Supervisor Prof. Lea-Der Chen. Ready from WWW: <`http://etd.lib.uiowa.edu/2006/mtinker.pdf`>.

[25] VAN GAAL, R. *Racer Car and Racing Simulator* [online]. [Netherland]: 2000-2009 , 27.1. 2009 [quot. 2009-03-12]. Ready from WWW: <`http://www.racer.nl/`>.

[26] VLK, F. *Dynamika motorových vozidiel.* 2nd edition. Brno: František Vlk, 2003. 434 p. ISBN 80-239-0024-2.

[27] VLK, F. *Převody motorových vozidel.* 1st edition. Brno: František Vlk, 2006. 371 p. ISBN 80-239-6463-1.

[28] YANAKIEV, D, KANELLAKOPOULOS, I. *Engine and Transmission Modeling for Heavy-Duty Vehicles.* [s.l.]: [s.n.], 1995. 52 p. Institute of transportation studies University of California, Berkeley. Ready from WWW: <`http://www.path.berkeley.edu/PATH/Publications/PDF/TECHNOTES/TECH_NOTE_95-06.pdf`>.

[29] ZACKRISSON, T. *Modeling and simulation of a driveline with an automatic gearbox.* [s.l.], 2003. 68 p. Royal Institute of Technology. Thesis leader Johnny Arne. Ready from WWW: <`http://www.s3.kth.se/~kallej/grad_students/zachrisson_thesis03.pdf`>.

[30] ZHANG, R. *Multivariable robust control of nonlinear systems with aplication to an electro-hydraulic powertrain.* [s.l.], 2002. 217 p. University of Illinois at Urbana-Champaign. Doctoral thesis leader Prof. Andrew Alleyne. Ready from WWW: <`http://mr-roboto.me.uiuc.edu/evps/theses/rzhang_phd/rzhang_phd.pdf`>.
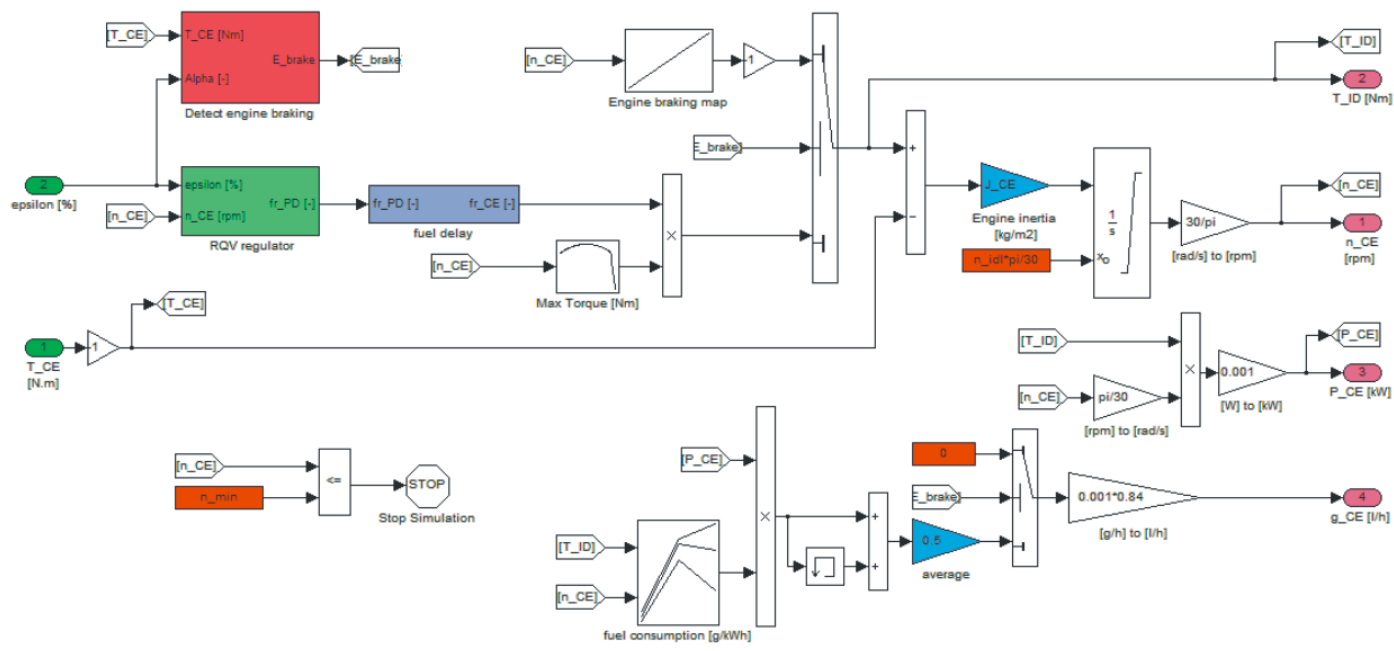
A Appendix

A.1 Simulink models
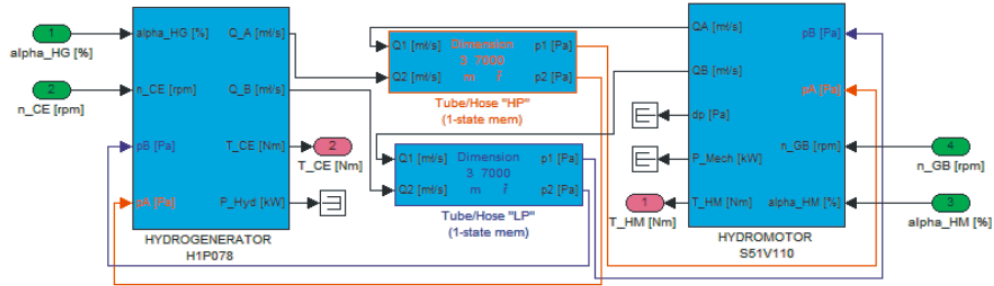
Figure A.1: Diesel engine model in Simulink

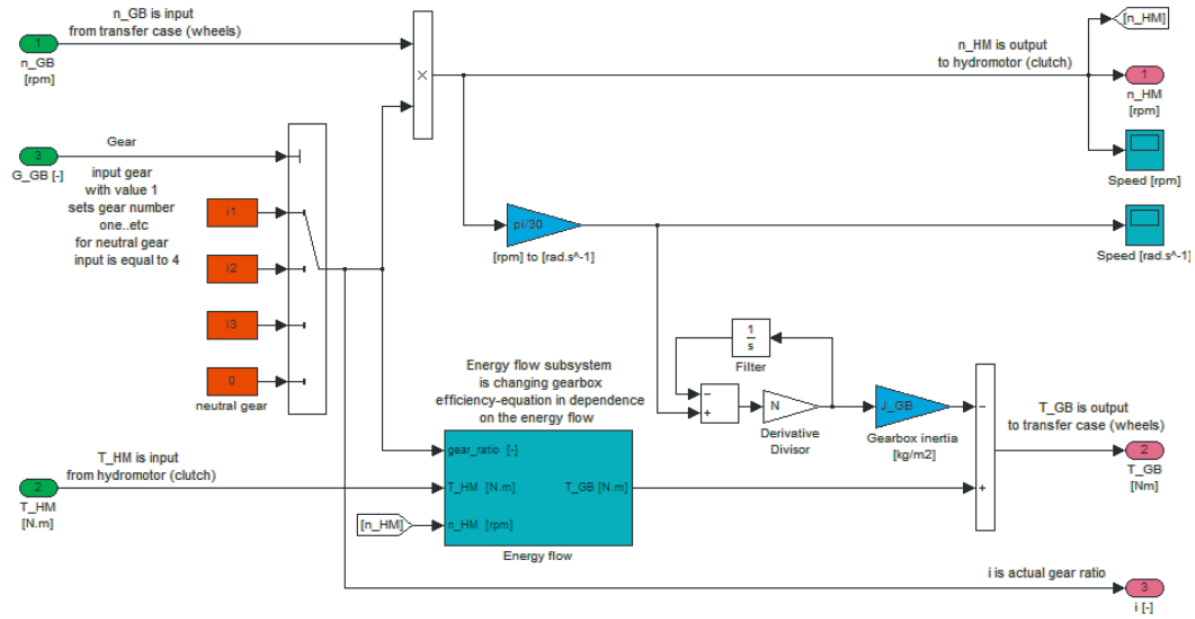Figure A.2: HST model in Simulink (Sauer-Danfoss)
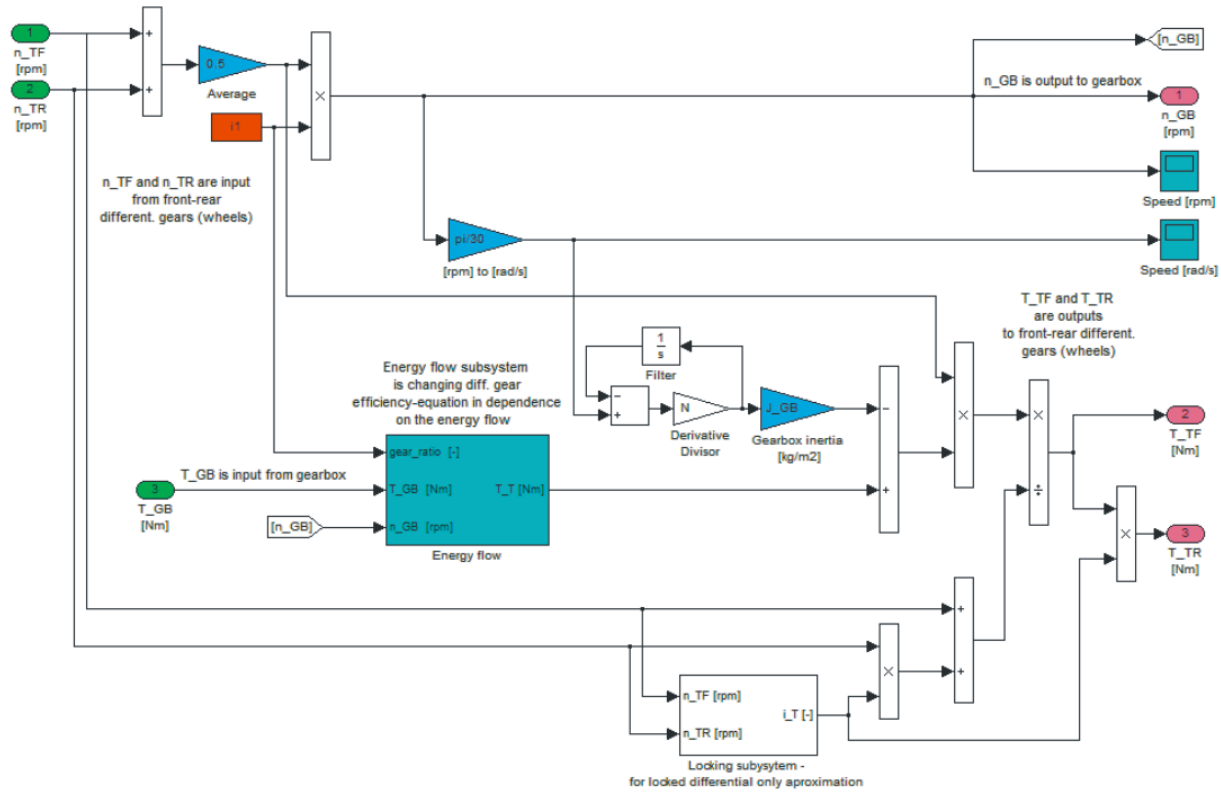
Figure A.3: Gearbox model in Simulink
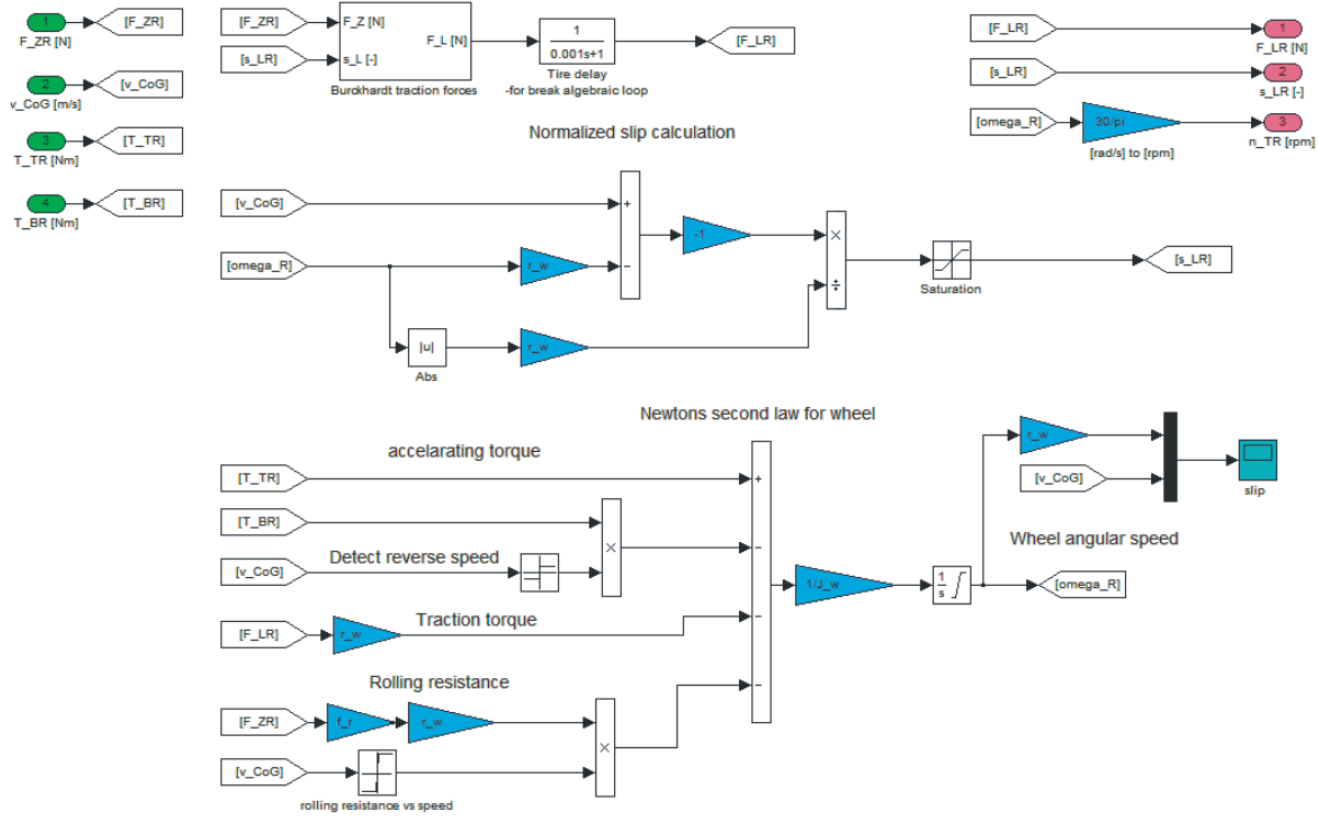
Figure A.4: Central differential gear model in Simulink
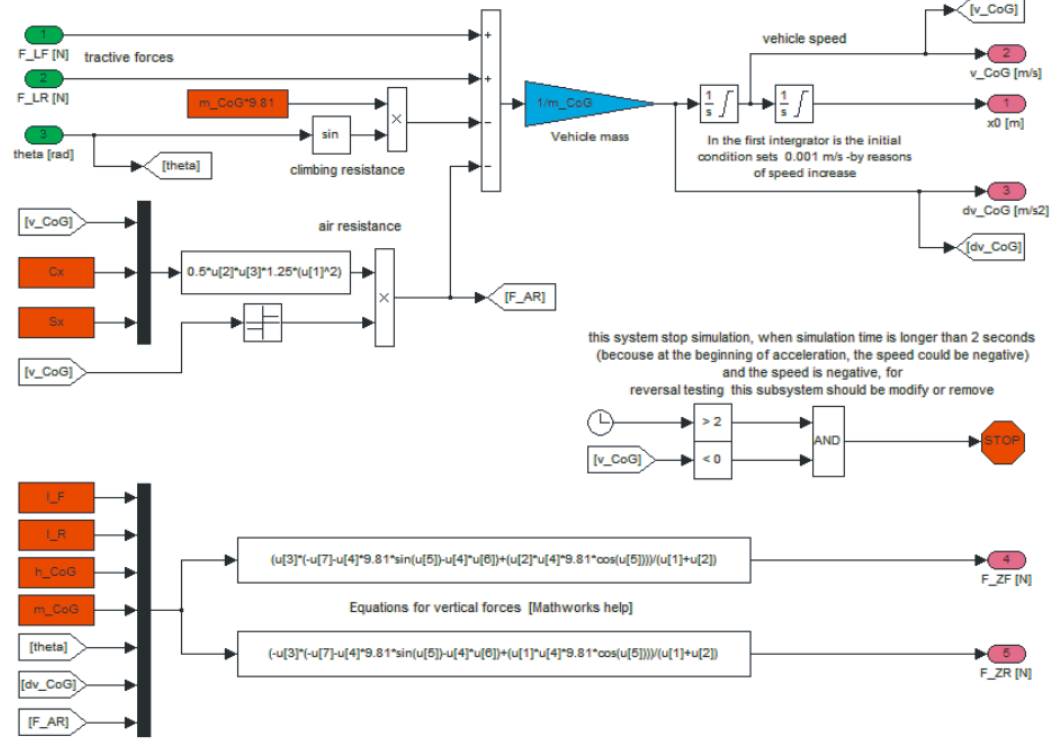
Figure A.5: Wheel model in Simulink

Figure A.6: Car body in Simulink

Figure A.7: HST control in Simulink
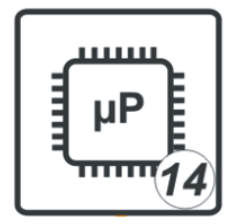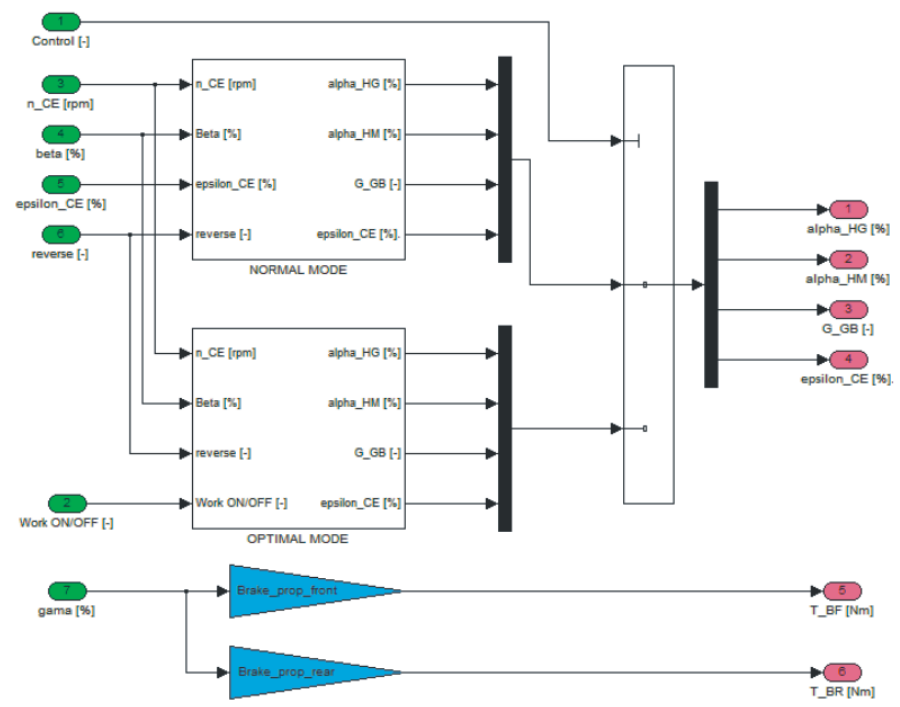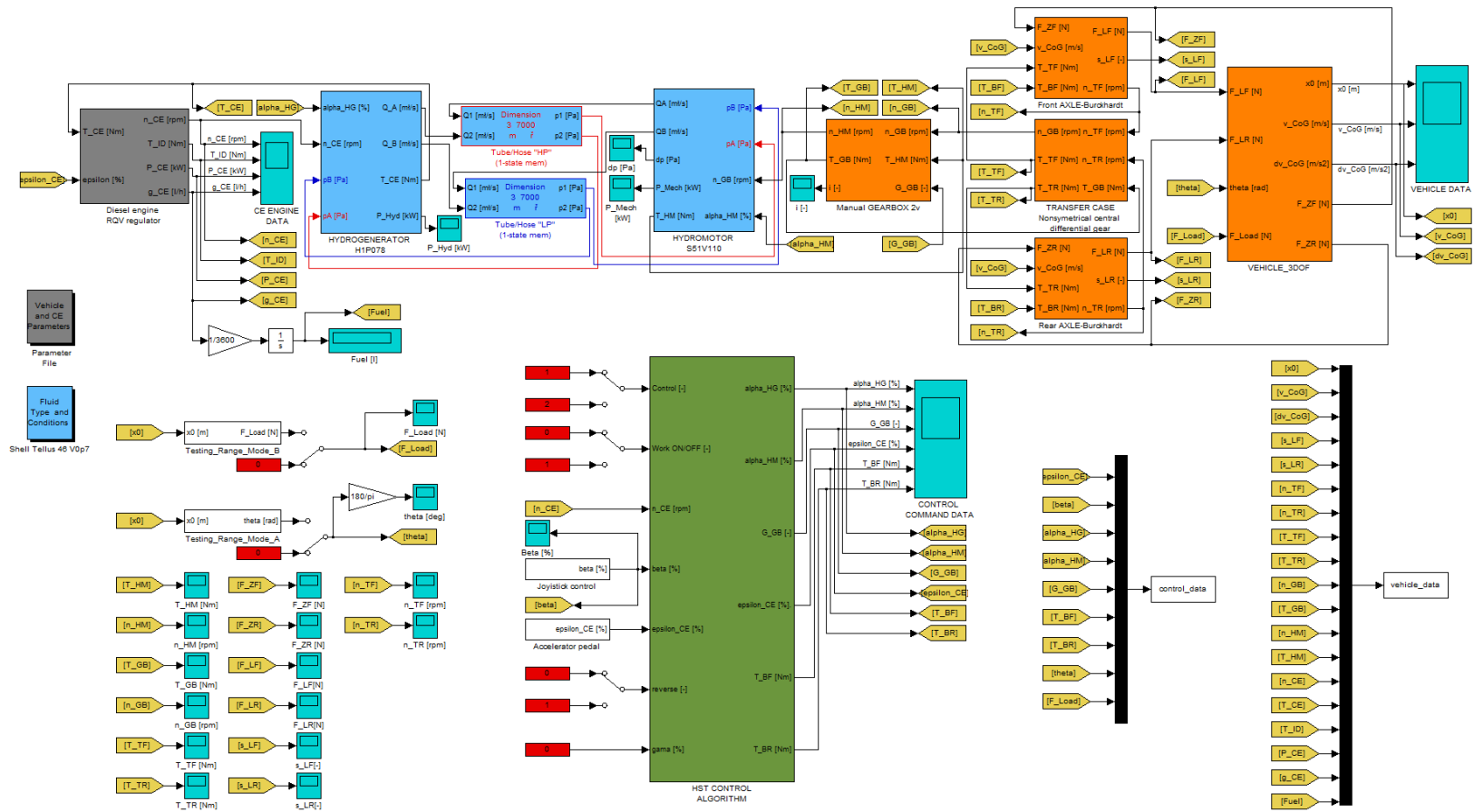
Figure A.8: Complex vehicle model in Simulink

A.2 Simulation parameters

VEHICLE PARAMETERS		
Vehicle mass	kg	7000
Vehicle load	kg	500
Loading resistance	N	2000
Distance from front axle to CoG	m	1.5
Distance from rear axle to CoG	m	1.5
Height of CoG	m	0.7
Air resistance coefficient	-	0.9
Cross sectional area of vehicle	m^2	5
WHEEL PARAMETERS		
Surface type (approximation)	-	asphalt wet
Rolling resistance	-	0.05
Wheel radius	m	0.5
Wheel/axle moment of inertia	$kg \cdot m^2$	100
CENTRAL DIFFERENTIAL GEAR PARAMETERS		
Central differential gear ratio (final gear)	-	20
Front axle torque distribution	%	50
Rear axle torque distribution	%	50
Gear efficiency	-	0.9
GEARBOX PARAMETERS		
Gearbox gear ratio 1st	-	3.5
Gearbox gear ratio 2st	-	1
Gear efficiency	-	0.9
HST PARAMETERS		
Default setting	-	-
DIESEL ENGINE PARAMETERS		
Maximal CE power	kW	75
Maximal CE speed	min^{-1}	2400
Minimal CE speed	min^{-1}	650
Idling CE speed	min^{-1}	850
Minimal fuel consumption	$g \cdot kW^{-1} \cdot h^{-1}$	210
Engine moment of inertia	$kg \cdot m^2$	1
Fuel rack time delay	s	0.1
Maximal brake power	%	60
Minimal brake power	%	10

Table A.1: Used tunable parameters for simulations